TN-22

DATA REQUIREMENTS AND DATA PREPARATION FOR DAMBRK PROGRAMME

SATISH CHANDRA
DIRECTOR

STUDY GROUP

SATISH CHANDRA
M PERUMAL

NATIONAL INSTITUTE OF HYDROLOGY
JAL VIGYAN BHAVAN
ROORKEE-247667(UP) INDIA

1985-86

CONTENTS

LIST OF SYMBOLS

A_s	Reservoir water surface area in acres
b	Final bottom width of breach
C_d	Co-efficient of discharge of crest of dam
C_g	Co-efficient of discharge of gated spillway
C_s	Co-efficient of discharge of uncontrolled spillway
h_o	Initial elevation of water in reservoir
h_{bm}	Final elevation of breach bottom
h_d	Elevation of top of dam
h_f	Elevation of water when breach begins to form
h_g	Elevation of center of submerged gated spillway
h_s	Elevation of uncontrolled spillway crest
Q_r	Constant head independent discharge from dam
Z	Side slope of breach
τ	Failure time of breach in hours

LIST OF FIGURES

ABSTRACT

Planning and design requirements for a wide range of projects, such as emergency preparedness and location of nuclear power plants, have generated widespread interst in dam break floods analysis. Although much academic research have been accomplished on this topic, a generalised analytic technique for calcuating and routing of dam break floods in natural channels is rarely available. The U.S. National Weather Services DAMBRK programme is meant to serve this practical purpose. This note presents the data requirements for analysing the flood wave generated by dam failure using the DAMBRK programme, and also gives the details on how to prepare the data for executing the DAMBRK programme for a most practical case. The DAMBRK programme was developed so as to require data that is accessible to the forecaster. The input data can be categorised into two groups. The first data group pertains to the details of dam such as breach, spillways, and reservoir storage volume, etc. The second group pertains to the routing of the outflow through the downstream valley. The input data requirements are flexible in so far as much of the data may be ignored when a detailed analysis of a dam break flood inundation event is not feasible due to lack of data or insufficient data preparation time.

1.0 INTRODUCTION

Protection of the public from the consequences of dam failures has taken on increasing importance as population have concentrated in areas vulnerable to dam break disasters. This has created general interest in the dam safety analysis in recent years. The organisations which are responsible for the safety of dams should plan for preventive measures so that in the eventuality of dam failures the disaster will not struck the lives of the population living downstream.

One of the preventive measure in avoiding dam disaster is by issuing flood warning to the public of downstream when there is a failure of a dam. However, it is quite difficult to conduct analysis and determine the warning time regarding dam break flood at the time of disaster. Therefore, pre-determination of the warning time assuming a hypothetical dam break situation is a needed exercise in dam safety analysis. The method used for such analysis gains more credibility if one can simulate the past dam break failure scenario using that method with reference to failure mode and flood wave movement downstream of the dam.

Although many publications are available on dam break simulation problem since 1892 (Ritter, 1892) only a very few deal it with practical consideration. One of the unrealistic assumption made in many of those publication is that the dam fails completely and instantaneously. The assumptions are

somewhat appropriate for concrete arch type dams, but they are not appropriate for earthern dams and concrete gravity dams. Earthern dams which exceedingly outnumber all other types of dams do not tend to completely fail nor do they fail instantaneously. The breach requires a finite interval of time for its formation through erosion of the dam materials by the escaping water.

1.1 DAMBRK Programme

The U.S. National Weather Service (NWS), after taking into consideration the practical aspects of dam failure condition and subsequent flood wave movement, has developed (Fread, 1977) and improved (Fread, 1984) a computer programme 'DAMBRK' for the purpose of forecasting downstream flooding with reference to flood inundation information and warning times resulting from dam failures.

1.1.1 Purpose of DAMBRK programme

DAMBRK programme simulates the failure of a dam, computes the resultant outflow hydrograph and simulates movement of the dam-break flood wave through the downstream river valley. Two or more dams in series can also be accommodated. The results of these computations can be used to develop potential inundation maps for hypothetical and historical failures, establish time of travel of various portions of the flood wave to downstream locations and evaluate the effects of uncertainties in the dam failure paramters on these quantities. The analysis may be done for existing structures or those in

planning or design stages. The theoretical description of the DAMBRK programme as given by Fread (1984) is reproduced in Appendix-I.

1.1.2 Capabilities of DAMBRK programme

The DAMBRK programme has the capability of simulating a total of 12 different cases corresponding to a combination of various reservoir routing techniques and channel flood routing techniques in the presence of a single or multiple dams in river reaches. Some of these options take into consideration the routing of dam break flood wave through the downstream strauctures, like major bridges, with special internal boundary conditions.

1.2 Purpose of the Report

This report focusses data requirements and data preparation needed for DAMBRK programme. This also presents the description of the data input into each card along with the utility codes. The preparation of data in the programme required format is made for an option which is the most encountered one in practice. The modification required in the input data for other options of the programme are only slightly different from the considered one.

2.0 DATA REQUIREMENTS

The DAMBRK model was developed so as to require data that was accessible to the forecaster. The input data requirement are flexible in so far as much of the data may be ignored (left blank on the input data cards or omitted altogether) when a detailed analysis of a dam break flood inundation event is not feasible due to lack of data or insufficient data preparation time. Nontheless the resulting approximate analysis is more accurate and convenient to obtain than that which could be computed by other techniques. The input data can be categorized into two groups.

The first data group pertains to the dam (the breach spillways, and reservoir storage volume). The breach data consists of the following parameters: (failure time of breach, in hours), b (final bottom width of breach), $\bar{z}$ (side slope of breach), h_{bm} (final elevation of breach bottom), h_o (initial elevation of water in reservoir), h_f (elevation of water when breach begins to form), and h_d (elevation of dam). The spillway data consists of the following: h_s (elevation of uncontrolled spillway crest), C_s (coefficient of discharge of uncontrolled spillway), h_g (elevation of center of submerged gated spillway), C_g (coefficient of discharge of gated spillway), C_d (coefficient of discharge of crest of dam), Q_t (constant head independent discharge from dam). The storage parameters consist of the following: a table of surface area (A_s) in acres or volume in acre ft. and the corresponding elevations within the reservoir. The

forecaster must estimate the values of τ, b, $\mathcal{Z}$, h_{bm}, and h_f. The remaining values are obtained from the physical description of the dam, spillways, and reservoir. In some cases h_s, C_s, h_g and C_g and C_d may be ignored and Q_t used in their place.

The second group pertains to the routing of the outflow hydrograph through the downstream valley. This consists of a description of the cross-sections, hydraulic resistance coefficients, and expansion coefficients. The cross-sections are specified by location milage, and tables of top width (actaive and inactive) and corresponding elevations. The active top widths may be total widths as for a composite section , or they may be left floodplain, right flood plain, and channel widths. The channel widths are usually not as significant for an accurate analysis as the overbank widths. The number of cross-sections used to describe the downstream valley depends on the variability of the va lley widths. They also depend on the availability of cross-section measurements. However, a minimum of two must be used. Additional cross-sections are created by the model via linear interpolation between adjacent cross-sections specified by the forecaster. This feature enables only a minimum of cross-sectional data to be input by the forecaster according to such criteria as data availability, variation, preparation time etc. The number of interpolated cross-sections created by the model is controlled by the parameter DXM which is input for each reach between specified

cross-sections. The expansion-contraction coefficients (FKC) are specified as non-zero values at sections where significant expansion or contractions occur. But they may be left blank in most analyses.

3.0 DATA PREPARATION

The accuracy with which the dam **break** simulation can be made depends on the fidelity with which breach parameters, flow, geometry and roughness are respresented. This section focusses on how breach simulation parameters, flow geometry and roughness are defined in DAMBRK programme. In addition the input data structure along with the utility codes is presented for using DAMBRK.

3.1 Representation of Breach Formation

Two types of breaching may be simulated using this programme:

1. An overtopping failure in which the breach is simulated as a rectangular, triangular, or trapezoidal shaped opening that grows progressively downward from the dam crest with time. Flow through the breach at any instant is calculated using a broad crested weir equation.
2. A piping failure in which the breach is simulated as a rectangular orifice that grows with time and is centered at any specified elevation within the dam. Instantaneous flow through the breach is calculated with either orifice or weir equations depending on the relation between pool elevation and the top of the orifice.

During the simulation of a dam failure, the actual breach formation commences when the reservoir water surface elevation (h) exceeds a specified value, h_f. This feature permits the simulation of an overtopping of a dam in which the breach does not form until a sufficient amount of water is flowing over the crest of the dam. A piping failure may be simulated when h_f is specified less than the height of the dam, h_d. The description of these two types of breach formation along with the concerned parameters is given below:

3.1.1 Formation of breach due to overtopping

Figure 1 shows the front view of dam showing formation of breach due to overtopping.

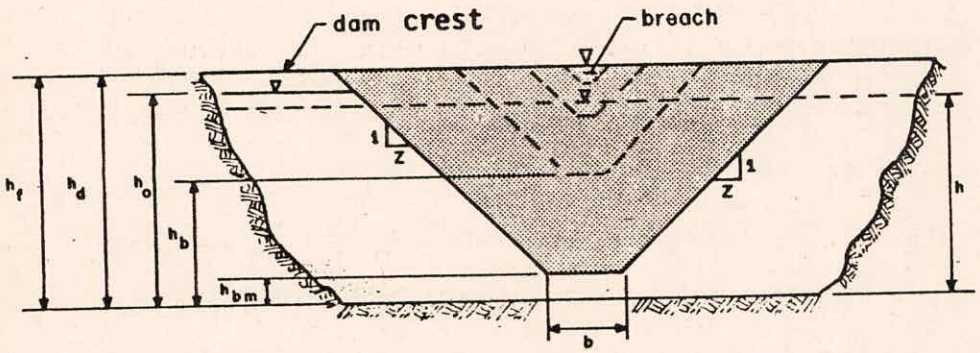

Figure. 1 FRONT VIEW OF DAM SHOWING FORMATION OF BREACH

For reasons of simplicity, generality, wide applicability and the uncertainty in the actual failure mechanism, the DAMBRK programme allows the forecaster to input the failure time interval (τ) and the terminal size and shape of the breach. The shape is specified by a parameter (Z) identifying the side slope of the breach i.e. 1 vertical Z horizontal slope The range of Z values is $0 \leq Z \leq 2$. The final breach size is controlled by the Z parameter and another parameter (b) which is the terminal width of the bottom of the breach Rectangular, triangular or trapezoidal shapes may be specified for the description of the breach For example, $Z = 0$ and $b > 0$ produces a trapezoidal shape. As shown in figure 1, the model assumes the breach bottom width starts at a point and enlarges at a linear rate over the failure time interval (τ) until the terminal width is attained and the breach bottom has eroded to the elevation h_{bm} which is usually, but not necessarily the bottom of the reservoir or outlet channel bottom. If τ is less than 10 minutes, the width of the breach bottom starts at a value of b rather than at a point. This represents more of a collapse failure than an erosion failure.

3.1.2 Formation of breaching due to piping

If the specified elevation, h_f that triggers formation of breach is below the crest of the dam, a piping failure is simulated. In this case, the breach is rectangular and grows as depicted in figure 2.

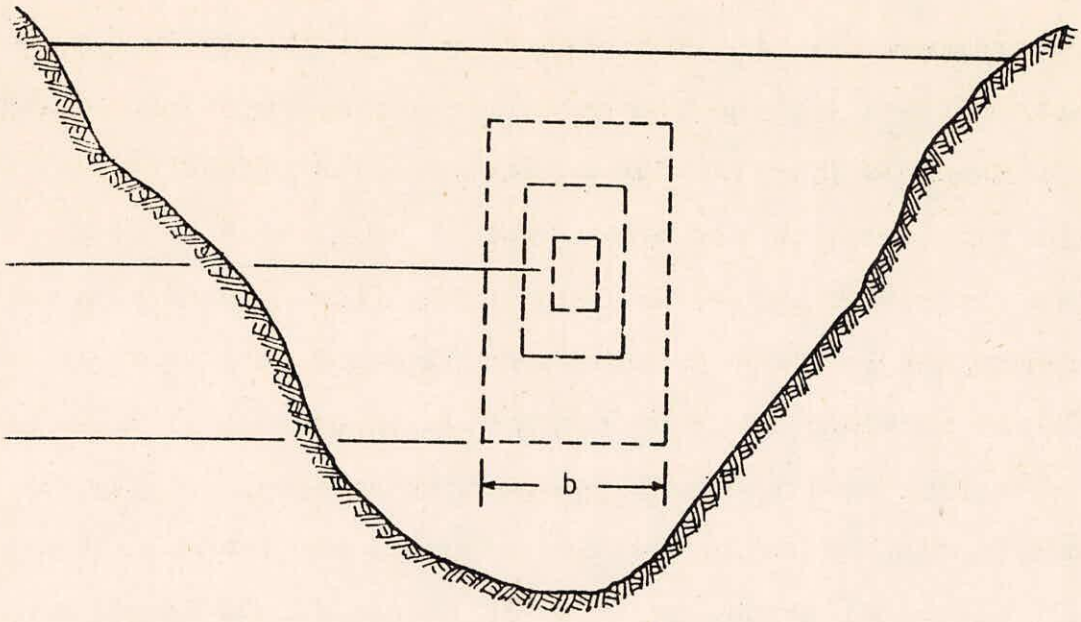

Figure 2 ORIFICE BREACH

3.2 Representation of Data of Spillways and Reservoir Storage Volume

The representation of data ,as described in section 2.0, pertaining to spillway and reservoir storage volume are straight forward and are readily available in practice.

3.3 Preparation of Data on River Characteristics

Flow geometry and off-channel storage are represented in DAMBRK through means of user specified cross-sections. Cross-section location is specified in terms of river miles from the dam. Cross-sections should be positioned so as to best characterize the geometry of the anticipated flow

paths. They should extend across the valley with a liberal allowance for the maximum anticipated depths of flow. Cross section alignment should always be perpendicular to the anticipated flow lines, which may require a dog-leg or curvilinear alignment.

A cross section is defined in terms elevation and widths. The same number of elevations should be used for each cross section, a maximum of eight is permitted. Widths for elevations greater than maximum elevation supplied by the user are obtained by linear extrapolation. For each elevation for a cross section, two widths may be specified - an 'active flow' width and an 'inactive' (or off-channel storage) width. It is presumed that flow through the active flow portion of a cross section is normal to the plain of the cross section with a velocity that can be appropriately represented with Manning's equation. Only the active flow portion of a cross section is considered in defining terms in the momentum equation.

The inactive portion of a cross section is intended to account for an area where water ponds and/or does not have a significant velocity component in the direction of flow. Characteristics of the total cross section, active plus inactive are reflected in the terms of the continuity equation. Figure 3 illustrates representation of a cross section with elevation and widths that has both active and inactive areas.

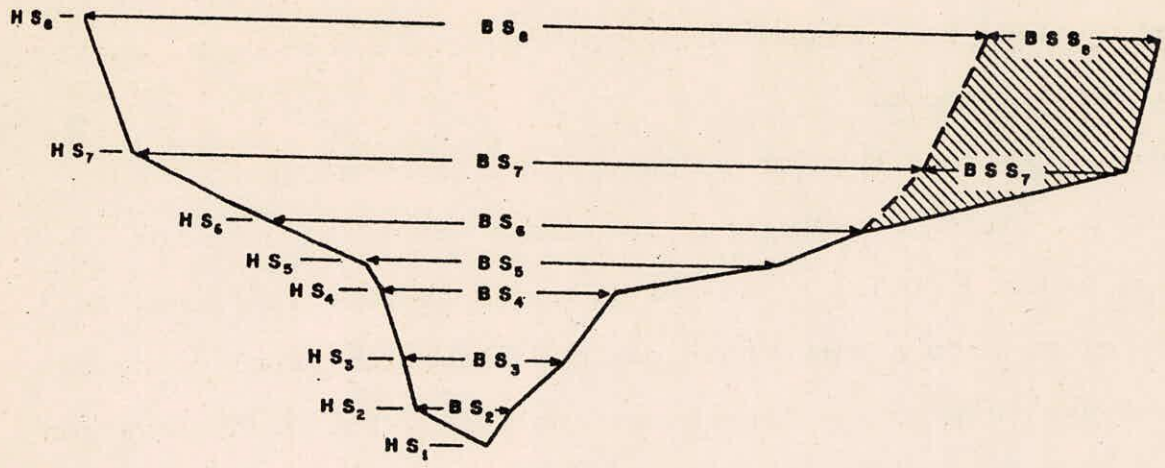

Figure 3- CROSS SECTION REPRESENTATION

Off channel storage, for example on a tributary, can be modelled by locating three cross sections as shown in figure 4, and developing off-channel storage widths to reflect storage in the tributary. The widths can be calculated for the middle cross section as follows:

$$BSS = \frac{2\ (SA)}{L}$$

where,

BSS - Off-channel storage width in ft. for middle cross section at elevation E ft.

SA - Surface area of off-channel storage in square ft. at elevation E ft.

L - Distance in ft. between first and third cross-sections.

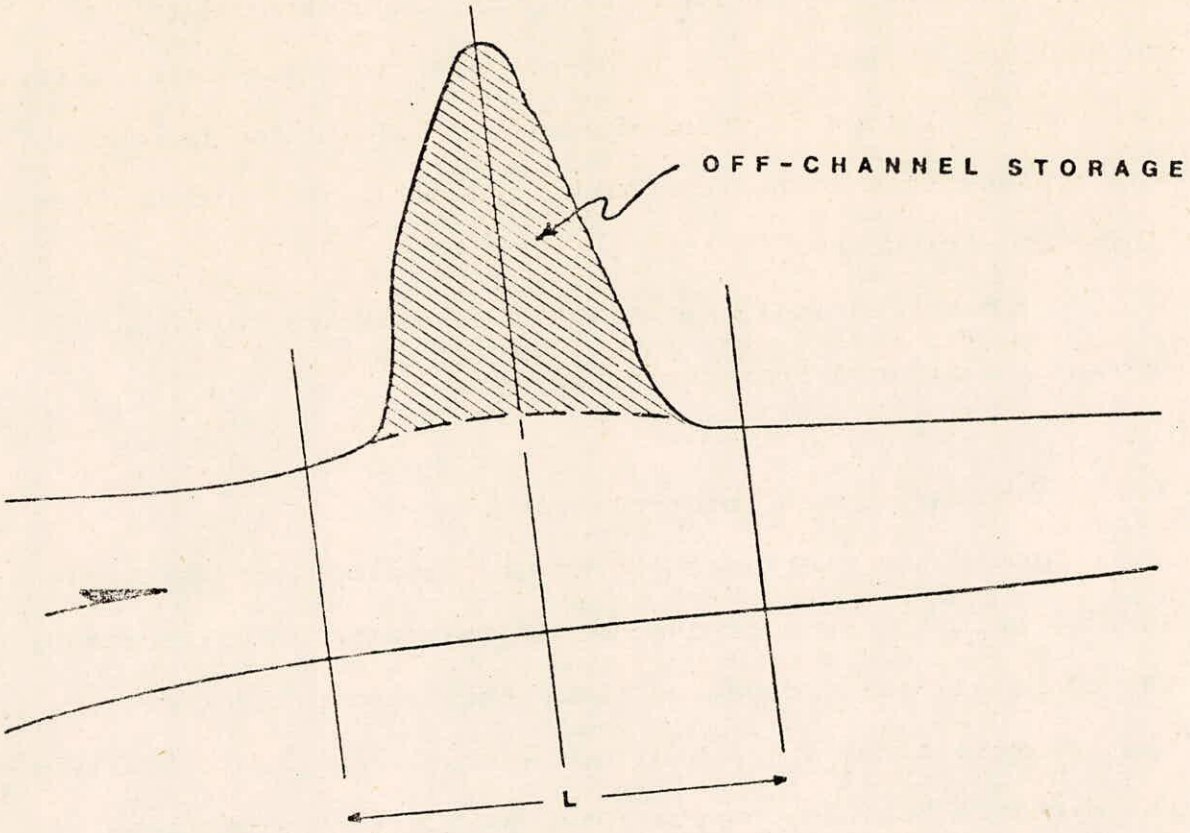

Figure 4 - OFF-CHANNEL STORAGE (PLAN VIEW)

Implicit in this treatment of off-channel storage is the assumption that the time required to occupy and evacuate it is negligible. This assumption would not be valid for a long tributary for which filling and draining times are significant relative to the time required for the flood wave to pass the mouth of the tributary. Filling and draining of a long tributary can be more accurately treated using two applications of the model. In the first, the dam failure is simulated and the wave is routed to the confluence of the

tributary. A second application of the model routes flow through the tributary and on downstream along the main river. The dam-break flow is entered as a lateral inflow hydrograph which propagates downstream along the main river and upstream along the tributary.

Cross-sectional data in X- Y co-ordinate format at commonly available from field surveys.

3.3.1 Cross-section interpolation

Apart from the necessity to give appropriate definition to flow geometry and off-channel storage with cross-sections, the computational procedures themselves impose requirements that constrain the spacing of cross-sections. Theoretically, the distance between computational points (cross-sections) should equal the distance travelled by the flood wave during a computation interval. Because both the flood wave velocity and the computation interval vary during a simulation, the theoretical criteria can only be approximately satisfied. Flood wave velocity increases with the depth of flow, hence relatively short distance steps are required near the failing dam, and steps can be lenghtened with increasing distance from the dam as the flood wave attenuates. To meet these variable distance step requirements, DAMBRK contains capability to automatically interpolate cross-sections. The user specifies the maximum distance between computation points (cross-sections) for reach reach between input cross-sections. The programme will automatically interpolate cross-sections

to satisfy the criteria.

The cross-section interpolation procedure used by the programme performs linear interpolation of elevation and width with distance between adjacent cross-sections. This manner of interpolation, while computationally simple gives rise to the need for defining cross-sections on a consistent basis. Erroneous interpolation could occur when adjacent cross-sections are markedly dissimilar.

3.4 Roughness Representation

3.4.1 Application of roughness coefficients

Boundary resistance is reflected in the equation of motion through the friction slope, which is defined with Manning's equation. Friction slope is determined for a reach in terms of an arithmatic average of the hydraulic radii, for the 'effective flow' portions of cross-sections at each end of the reach. It is assumed that wetted perimeter is equal to the effective water surface width. This assumption results in negligible error if the width-to-depth ratio for effective flow is greater than a value of about 10. For narrow, deep cross sections, the wetted perimeter assumption can be accommodated by employing appropriately larger n-values.

3.4.2 Composite roughness

Manning's roughness coefficients (n-values) are specified for reaches containing two or more cross sections

as a set of composite n-values which vary with elevation or discharge. A composite n-value is an equivalent n-value associated with the entire (effective) wetted perimeter of a cross-section. The programme interpolates linearly in the table of composite n-values based on the average water surface elevation for the reach. If the average water surface elevation exceeds the average of the largest elevations specified for the cross-sections at each end of the reach, linear extrapolation is used to obtain the n-value. Typically n-values are specified with a lateral variation across the cross-section as shown in figure 5.

3.5 Expansion and Contraction Coefficients

The user must specify a value for the expansion or contraction coefficients for each reach where the expansion or contraction of channel section respectively is encountered. The value assigned by the user must be positive for a contraction and negative for an expansion. The contraction values vary from 0.1 to 0.3, the expansion value vary from -0.5 to -1.0. If contraction-expansion effects are negligible, zero values are entered.

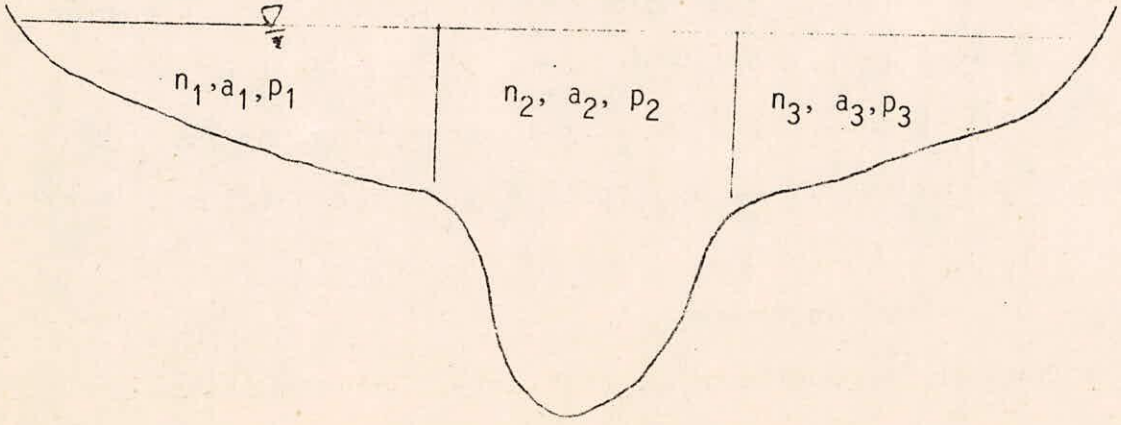

Figure 5 - LATERAL VARIATION OF n-VALUES ACROSS A CROSS-SECTION

4.0 INPUT DATA STRUCTURE FOR DAMBRK PROGRAMME

Input card group no.

(1) MDAM, MRVR, MNAME - 20 A 4 Format

MDAM	Name of dam (col. 1-20).
MRVR	Name of reservoir (col. 21-40).
MNAME	Agency name (col. 41-60).

MESAGE - 20 A 4 Format

MESAGE	Agency address--street, room (col. 1-40). Agency Address--city, state, zip code (col. 41-72).

(2) KKN, KUI, MULDAM, KDMP, ITEH, NPRT, KFLP, KSL - 8 I 10 Format

KKN	Parameter which is associated with KSUPC on card (16). If KSUPC=0, KKN=1; if KSUPC=1, KKN should be given a value of 1 if the downstream channel valley below the dam is entirely supercritical flow or KKN should be given a value of 2 if the downstream reach is divided into two reaches (an upstream reach having supercritical flow and a downstream reach having subcritical flow). If KKN=9, a hydrograph is read in and then routed through the downstream valley.
KUI	Parameter used to select type of reservoir routing for determining outflow hydrograph; if KUI=0, storage routing is used; if KUI=1, dynamic routing is used.
MULDAM	Parameter used to select option for routing through multiple reservoirs sequentially located downstream of first dam. If one or more dams are located downstream of first dam, MULDAM=1, if no dams are downstream of first dam, then MULDAM=0. Any number of downstream sequentially located dams may be simulated by letting KKN=1 + no. of downstream dams.
KDMP	Parameter for printing; users outside of the National Weather Service set KDMP=3. KDMP=0, print only title page; KDMP=1, title page, abstract, variable descriptions; KDMP=2, same as KDMP=1 plus input data; KDMP=3, title page plus input data; KDMP=4, same as KDMP=2, then stop; if KDMP=5, IOPUT on card (4) allowing selective printout of computations is read-in and KDMP is reset to 3.

ITEH — Parameter denoting number of hydrograph ordinates of inflow hydrograph to reservoir; maximum value of 50 is allowed; if ITEH=0, the inflow hydrograph is generated via a mathematical function.

NPRT — Parameter to control print output for JNK=9, NPRT is the total number of cross-sections at which hydraulic information is printed-out during dynamic routing; if NPRT=0, the program uses a variable NPRT computed by the program and prints-out hydraulic information at NPRT intervals of cross-sections along the routing reach.

KFLP — Parameter denoting the use of the special flood-plain routing feature; if KFLP=0, the special flood-plain feature is not used; if KFLP=1, the special flood-plain routing is used.

KSL — Parameter denoting simulation of landslide; if KSL=0, no landslide; if KSL=1, a landslide occurring along one bank of the reservoir is simulated; if KSL=2, the landslide occurs along both banks of reservoir.

(3) NPT(K) - 8 I 10 Format

NPT(K) — Sequential number of cross-section at which hydraulic information is printed-out; this card is omitted if NPRT=0; K index goes from 1 to NPRT where NPRT $\leq$ 30.

(4) IOPUT(K) - 10 I 1, 2 I 2 Format

IOPUT(K) — Optional print parameter that may override the JNK parameter, (card 16). K index goes from 1 to 12. If IOPUT(K)=0, allow the output to be printed; if IOPUT(K)=1, suppress the output. The following output can be controlled:

Col	
1	Slope profile plot
2	Summary tables of input x.s. and reaches
3	Initial conditions table - flow and "L" tables (reversed)
4	Initial conditions table - backwater elevation table (forward)
5	Dynamic routing - at upstream and downstream boundaries
6	Dynamic routing - at each multiple dam site (similar to depletion table)
7	Summary plots - peak elevation, discharge, time to peak, and time to flood elevation
8	Arrays for selected hydrograph plots
9	List of input cross-sectional information
10	Reservoir depletion table

Col	
11-12	This value reperesents the time at which printing of output will commence. All output will be suppressed until this time is reach.
13-14	The interval at which the output will be printed.

Note: This information can only be controlled if the JNK parameter allowed it to be printed originally.

(5) IDAM(K) - 8 I 10 Format

IDAM(K)	Number of cross-section coincident with the upstream face of each dam; K index goes from 1 to MULDAM. This parameter is only read-in when the simultaneous computation of the complete system is desired (see note on page A-21 for further information on the use of this computational option).

(6) SA(K) - 8 F 10.0 Format

SA(K)	Surface area (acres) or volume (acre-ft) of reservoir at elevation HSA(K). If KUI=1 and KKN≠1 or KKN=9, omit card (6). Maximum of 8 values allowed.

(7) HSA(K) - 8 F 10.0 Format

HSA(K)	Elevation (ft) at which reservoir surface area SA(K) is defined; elevation is referenced to a datum plane corresponding to mean sea level (m.s.l.). If KUI=1 and KKN≠1 or KKN=9, omit card (7). Elevations start at highest and proceed to lowest. Maximum of 8 values allowed. Lowest elevation must be YBMIN as defined on card (8).

(8) RLM, YO, Z, YBMIN, BB, TFH, DATUM, VOL - 8 F 10.0 Format

RLM	Length (mi) of reservoir.
YO	Elevation (ft) of water surface in reservoir when computation commences; elevation is referenced to m.s.l. datum.
Z	Side slope (1:vertical to z:horizontal) of breach.
YBMIN	Lowest elevation (ft) that bottom of breach reaches; elevation is referenced to m.s.l. datum.

BB	Width (ft) of base of breach.
TFH	Time (hr) from beginning of breach formation until it reached its maximum size.
DATUM	Elevation (m.s.l.) of bottom of dam.
VOL	Parameter indicating if SA(K) is surface area (acres) or volume (acre-ft); if VOL=0.0, SA(K) is acres; if VOL=1.0, SA(K) is acre-ft.

(9) HF, HD, HSP, HGT, CS, CG, CDO, QT - 8 F 10.0 Format

HF	Elevation (ft) of water when failure of dam commences; elevation is referenced to m.s.l. datum; if HF is less than HD, the breach is formed by "piping."
HD	Elevation (ft) of top of dam; elevation is referenced to m.s.l. datum.
HSP	Elevation (ft) of uncontrolled spillway crest; elevation is referenced to m.s.l. datum.
HGT	Elevation (ft) of center of gate openings; elevation is referenced to m.s.l. datum.
CS	Discharge coefficient for uncontrolled spillway; it is equal to the coefficient of discharge (2.6-3.2) times the length (ft) of the spillway.
CG	Discharge coefficient for gate flow; it is equal to the coefficient of discharge (0.60-0.80) times the area of gates.
CDO	Discharge coefficient for uncontrolled weir flow over the top of the dam; it is equal to the coefficient of discharge (2.6-3.2) times the length of the dam crest (ft) less the length of the uncontrolled spillway and gates.
QT	Discharge (cfs) through turbines; this flow is assumed constant from start of computations until the dam is completely breached; thereafter, QT is assumed to be zero. QT may also be considered leaking or constant spillway flow.

Note: Omit cards (8) and (9) if KKN=9.

(10) QSPILL(K,L) - 8 F 10.0 Format

QSPILL(K,L)	Flow (cfs) of spillway or gate rating curve; K goes from 1 to maximum of 8; L goes from 1 to MULDAM (card (2)) which may be a maximum of 10; if MULDAM=0, L goes from 1 to 1.

(11) HEAD(K,L) - 8 F 10.0 Format

HEAD(K,L) Head (ft) above spillway crest or gate center; head is associated with spillway flow or gate flow in rating curve; K goes from 1 to maximum of 8; L goes from 1 to MULDAM.

Note: Repeat cards 10-11 as L index goes from 1 to MULDAM. If MULDAM=0, L index goes from 1 to 1.

Note: Cards (10) and (11) are read-in only if either HSP is non-zero and CS is zero, or HGT is non-zero and CG is zero. This option allows a rating curve to be used for either the uncontrolled spillway or submerged gate rather than an equation for each using a constant discharge coefficient as in Eq. (17).

(12) DHF, TEH - 2 F 10.0 Format

DHF Interval (hr) between QI(K) input hydrograph ordinates; enter 0.0 if intervals are not equal.

TEH Time (hrs) from beginning of routing until routing is terminated.

(13) QO, RHO, GAMA, TPG - 4 F 10.0 Format

QO Initial steady discharge (cfs).

RHO Ratio of peak flow to initial flow of inflow hydrograph.

GAMA Ratio of time from initial steady flow to center of gravity of inflow hydrograph to time to peak of inflow hydrograph.

TPG Time from initial flow to peak flow of inflow (hr).

Note: Omit card 13 if ITEH (card 2) is nonzero.
If card 13 is included, then omit cards (14) and (15).

(14) QI(K) - 8 F 10.0 Format

QI(K) Inflow (cfs) at upstream end of reservoir for each interval of time during the failure and until time TEH is reached; K goes from 1 to ITEH which can assume a maximum value of 50; if ITEH=0, omit this card.

(15) TI(K) - 8 F 10.0 Format

TI(K) Time associated with QI(K) inflows; if DHF (card 12) is non-zero, or if ITEH (card 2) is equal to zero, omit this card, K goes from 1 to ITEH.

(16) NS, NCS, NTT, JNK, KSA, KSUPC, LQ, KCG - 8 I 10 Format

NS Number of cross-sections used to describe the channel and valley downstream of dam; first cross-section should be immediately downstream of dam; last cross-section should be at farthest point downstream of dam where flood information is desired; other cross-sections can be located as desired by user; maximum of 90 and minimum of 2 cross-sections can be used to describe the downstream channel valley.

NCS Maximum numer of top widths used to describe a cross-section.

NTT Total number of cross-sections at which discharge hydrographs will be plotted; maximum number is limited to 6. The location of the cross-sections at which plots are provided is specified by the parameter NT(K), which is on card (17). If NTT=0, no plots are provided. If NTT=a negative value between 1 and 6, the profile plots are suppressed.

JNK Parameter to specify the type of output other than plots which will be provided; if JNK=0, a minimum of output is provided—this includes all input data and hydrograph plots; if NTT=0, no hydrographs or other output printed; if JNK=1, reservoir depletion table printed, profile of downstream crests and times, and designated hydrographs; if JNK=4, additional information is printed at each time step for debugging; if JNK=9, information is printed for debugging.

KSA Parameter to enable downstream channel-valley cross-sections to be specified by a surface area vs. elevation table similar to the SA(K) and HSA(K) values described above; if KSA=1, downstream channel-valley cross-sections will be described by input data consisting of a single table of surface area vs. elevations as indicated for cards (24) and (25); if KSA=0, this option is not used.

Also, a parameter to indicate type of cross section smoothing. If KSA<0, then smoothing of cross sections will be automatically performed. Type of smoothing is specified on card (18).

KSUPC — Parameter to indicate if flow is supercritical. If KSUPC=0, flow through entire downstream channel-valley reach is subcritical and no special treatment is required; if KSUPC=1, the flow is known to be supercritical in either an upstream portion of the downstream channel-valley or throughout the entire downstream reach. When flow is supercritical, special computational procedures are used within the program. If only the upstream portion of the reach has supercritical flow, two sets of downstream channel-valley inputs commencing with card no. (16) are read in.

LQ — Parameter denoting the total number of lateral inflow hydrographs along the downstream channel-valley; a maximum of 10 hydrographs, each with 50 ordinates, are allowed.

KCG — Number of ordinates in spillway gate control curve of gate coefficient (CGCG) vs. time (TCG) described on cards (56) and (58). If KCG is negative, it is the total number of floodplain compartments. Maximum of 16 allowed.

Note: For debugging, JNK=4 or 9 is preferred.

(17) NT(K) - 6 I 10 Format

NT(K) — Number of cross-section (1 through NS) at which hydrograph plots are desired; K goes from 1 to NTT: if NTT=0, card no. (17) is omitted.

(18) SMF, NTSM, NSMR - F10.2, 2 I 10

SMF — Smoothing factor, $0.5 \leq SMF \leq 0.9$.

NTSM — Parameter indicating type of smoothing. If NTSM=1, smoothing of widths along x-axis; if NTSM=2, smoothing of widths in vertical where maximum width/ft change is |KSA|*50; if NTSM=3, smoothing of elevations along x-axis; NTSM=4, type 1 and type 2 smoothing; if NTSM=5, type 1, 2, and 3 smoothing.

NSMR — Number of separate smoothing reaches within the total routing reach.

(19) NUSM(K), NDSM(K) - 2 I 10

NUSM(K) — Upstream cross section number of K^{th} smoothing reach.

NDSM(K) — Downstream cross section number of K^{th} smoothing reach.

Note: Card (19) is read-in for each K^{th} smoothing reach as K goes from 1 to NSMR.

Note: Omit cards 18 and 19 if KSA $\geq$ 0 (card 16)

(20) XS(I), FSTG(I), XSL(I), XSR(I) - 4 F 10.0 Format

XS(I)	Location (mi) of cross-sections used to describe downstream channel-valley; mileage must increase in the downstream direction from dam. If KFLP=1 (card (2)), XS(I) is mileage measured along center of channel.
FSTG(I)	Elevation (m.s.l.) at which flooding commences; may be left blank.
XSL(I)	If KFLP=0, leave blank; if KFLP=1, XSL(I) is the mileage (location) of the I^{th} cross-section along the left (looking upstream) flood-plain.
XSR(I)	If KFLP=0, leave blank; if KFLP=1, XSR(I) is the mileage (location) of the I^{th} cross-section along the right flood-plain.

(21) HS(K,I) - 8 F 10.0 Format

HS(K,I)	Elevation (ft), referenced to m.s.l. datum, corresponding to each top width (BS(K,I)) on card (22) used to describe cross-section; K goes from 1 to NCS; NCS values of HS(K,I) are punched on a single card. NCS is limited to a maximum of 8. Start with lowest HS and proceed to highest value of HS.

(22) BS(K,I) - 8 F 10.0 Format

BS(K,I)	Top width (ft) of active flow portion of channel-valley cross-section corresponding to each elevation HS(K,I); K goes from 1 to NCS; NCS values of BS(K,I) are punched on a single card; NCS is limited to maximum of 8. This card is omitted if KSA=1.

(23) BSL(K,I) - 8 F 10.0 Format

BSL(K,I)	Top width (ft) of active flow portion of left flood-plain corresponding to each elevation HS(K,I); K goes from 1 to NCS; NCS values of BSL(K,I) are punched on a single card; NCS is limited to a maximum of 8. This card is omitted if KFLP=0 (card (2)).

(24) BSR(K,I) - 8 F 10.0 Format

BSR(K,I) Top width (ft) of active flow portion of right flood-plain corresponding to each elevation HS(K,I). This card is omitted if KFLP=0.

(25) BSS(K,I) - 8 F 10.0 Format

BSS(K,I) Top width (ft) of off-channel storage portion of channel-valley cross-section corresponding to each elevation HS(K,I); K goes from 1 to NCS; NCS values of BSS(K,I) are punched on a single card; NCS is limited to maximum of 8; this card is omitted if KSA=1 (card (16)).

(26) DSA(K,I) - 8 F 10.0 Format

DSA(K,I) Surface area (acres) of active flow portion of down-stream channel-valley cross-section corresponding to each elevation HS(K,I); K goes from 1 to NCS; NCS values of DSA(K,I) are punched on a single card; NCS is limited to maximum of 8; this card is omitted if KSA < 0.

(27) SSA(K,I) - 8 F 10.0 Format

SSA(K,I) Surface area (acres) of off-channel storage portion of channel valley cross-section corresponding to each elevation HS(K,I); K goes from 1 to NCS; NCS values of SSA(K,I) are punched on a single card; NCS is limited to maximum of 8; this card is omitted if KSA=0.

Note: Cards (20)-(25) are repeated for each cross-section as in the index I goes from 1 to NS.
When KSA=1, the cards are read-in as follows: (20), (21), (26), (27), (20), (21); this option is limited to the case of NS=2.

(28) CM(K,I) - 8 F 10.0 Format

CM(K,I) Manning n for channel corresponding to each elevation HS(K,I); K goes from 1 to NCS: NCS values of CM(K,I) are punched on a single card; NCS is limited to maximum of 8; the Manning n represents the roughness enountered by the flow through the reach bounded by cross-sections at locations I and I+1.

(29) CML(K,I) - 8 F 10.0 Format

CML(K,I) Manning n for left flood-plain corresponding to each elevation HS(K,I); K goes from 1 to NCS; NCS values of CM(K,I) are punched on a single card; NCS is limited to a maximum of 8. This card is omitted if KFLP=0 (card 2).

(30) CMR(K,I) - 8 F 10.0 Format

CMR(K,I) Manning n for right flood-plain corresponding to each elevation HS(K,I). This card is omitted if KFLP=0.

Note: Cards (28, 29, 30) are repeated for (NS-1) reaches.

(31) DXM(I) - 8 F 10.0 Format

DXM(I) Minimum Δx distance (mi) between cross-sections used in the computations. If DXM(I) is less than the distance between two adjacent cross-sections among the NS cross-sections read in, then intermediate cross-sections are created within the program via an interpolation procedure. (NS-1) values of DXM(I) are punched on one or more cards (8 values to a card); maximum no. of DXM(I) values is limited to 89; values assigned to DXM(I) should not result in more than 200 cross-sections produced by the interpolation procedure. (DXM values should be determined by the relationship C times Δt, where C is the approximate speed of the flood wave.)

(32) FKC(I) - 8 F 10.0 Format

FKC(I) Contraction-expansion coefficient; contraction values vary from 0.1 to 0.3, expansion values vary from -0.5 to -1.0; if contraction-expansion effects are negligible, enter 0.0 for FKC(I); (NS-1) values of FKC(I) are punched on one or more cards (8 values to a card); maximum no. of FKC(I) values is limited to 89.

(33) QMAXD, QLL, DTHM, YDN, SOM, FII, EPSY, TFI - 8 F 10.0 Format

QMAXD	Estimated maximum discharge (cfs) at downstream extremity of channel-valley reach; can be read in as 0.0 for initial run; subsequent runs can have a value of QMAXD as determined by the routing computations during the initial run. Only required when QLL is non-zero.
QLL	Maximum lateral outflow (cfs/ft) producing the volume losses experienced by the passage of the dam-break flood wave through the downstream valley; QLL has a negative sign and is computed by Eq. (63) in paper.
DTHM	Initial Δt time step size (hr); if 0.0 is read in, the value of DTHM is computed by the program; if DTHM<0.0, DTHM represents the divisor MDT for determining the time step (DTH=TFH/MDT) and DTHM is reset to zero. See note on page A-23.
YDN	Initial elevation of water surface at downstream end of routing reach; if channel control exists at this location, enter 0.0; YDN is non-zero if a dam or other control structure exists at the downstream end of the routing reach; if YDN=0.25, a single value rating curve of water surface elevation (m.s.l.) vs. discharge exists at downstream end; if YDN=0.5, critical flow such as waterfall exists at downstream end; if YDN=0.75, a specified water surface elevation (m.s.l.) such as a tide exists at the downstream end; if YDN=1.0, channel control exists at downstream end, but this signals the program that initial water surface elevations will be read-in at the NS cross-sections via card (48).
SOM	Slope of downstream channel (ft/mi) for first mile below dam.
FII	Theta (θ) weighting factor in finite difference solution; if left blank, a value of 0.60 is used in program; if 0.5 is used, θ is set internally to 0.60 and the model is capable of allowing negative flows to occur; if 0.51 is used, θ is set internally to 0.60 and the model routing is done by the diffusion method instead of dynamic routing.
EPSY	Convergence criterion for stage (ft) in Newton-Raphson iterative solution of finite difference unsteady flow equations; varies from .01 to .1 ft; if left blank, program use 0.01 ft. Also, can be used to specify the exponent m used in Eq. 65 in the paper; if EPSY≤0.50, m=4; if EPSY>0.5, m=EPSY and EPSY is automatically set to 0.01.
TFI	Time (hr) when time step changes from DTHM to TFH/MDT. See time step note on page A-23.

(34) NPLD - I 10

NPLD	Number of last floodplain compartment on same side of river where first floodplain compartment (FPC) is located; if no flow is transferred from one FPC to an adjacent FPC, let NPLD=0. Omit this card if KCG=0.

(35) NPXI(K), NQLP(K), PWELV(K), PCWR(K), PEO(K), QMINP(K) - 2 I 10, 4 F 10.0

NPXI(K)	Number of cross section immediately upstream of Δx reach where inflow to K^{th} FPC occurs.
NQLP(K)	Parameter indicating if pump discharge within the K^{th} FPC will be specified by a discharge hydrograph; 0 if no, 1 if yes.
PWELV(K)	Average elevation (ft. msl) of crest of weir (levee) along Δx reach where inflow to K^{th} FPC occurs.
PCWR(K)	Coefficient of discharge for weir flow along Δx reach where inflow to K^{th} FPC occurs; ranges in value from 2.6 to 3.2.
PEO(K)	Initial elevation (ft. msl) of water surface in K^{th} FPC at time = 0.
QMINP(K)	Minimum discharge (cfs) of total number of pumps in K^{th} FPC at all times.

(36) PSA(I,K) - 8 F 10.0

PSA(I,K)	Total volume (acre-ft) of K^{th} FPC below each elevation (PEL(I,K)); I index goes from 1 to 8.

(37) PEL(I,K) - 8 F 10.0

PEL(I,K)	Elevation (ft. msl) associated with each volume (PSA(I,K); elevations start at the lowest and proceed to the highest; I index goes from 1 to 8; last specified elevation should be greater than any expected water elevation within the FPC.

(38) QPU(I,K) - 8 F 10.0

QPU(I,K)	Inflow (cfs) to K^{th} FPC other than that transmitted over the weir (levee) from the main river; I index goes from 1 to ITEH (card no. 2).

(39) QLP(I,K) - 8 F 10.0

QLP(I,K) Specified total pump discharge (cfs) for K^{th} FPC; I index goes from 1 to ITEH (card no. 2); omit this card if NQLP(K)=0.

(40) COFF(I,K) - 8 F 10.0

COFF(I,K) Coefficient of discharge for flow over levee separating the K^{th} and $K^{th}+1$ FPC; coefficient is product of the broad-crested weir coefficient (2.6 to 3.2) and the length (ft) of the weir crest; the coefficient varies with elevation (HCFF(I,K)); I index goes from 1 to 8; omit this card if NPLD=0.

(41) HCFF(I,K) - 8 F 10.0

HCFF(I,K) Elevation (ft. msl) associated with the discharge coefficients (COFF(I,K)); elevations start at the lowest point along the levee crest and proceed upward; I index goes from 1 to 8; omit this card if NPLD=0.

Note Omit card no. 34 to 45 if KCG$\geq$0; otherwise repeat card no. 33 to 41 as K index goes from 1 to ABS(KCG).

(42) NPM - I 10

NPM Total number of pumps in all the FPC.

Note> Omit card no. 43 to 45 if NPM=0.

(43) IPMPL(L), NXPO(L), PEMN(L), PEMX(L) - 2 I 10, 2 F 10.0

IPMPL(L) Number of the K^{th} FPC in which the L^{th} pump is located.

NXPO(L) Number of the cross section immediately upstream of Δx reach where the L^{th} pump discharges into main river.

PEMN(L) Elevation (ft. msl) of water in K^{th} FPC when L^{th} pump starts pumping.

PEMX(L) Elevation (ft. msl) of water in K^{th} FPC when Lth pump stops pumping.

(44) DHP(I,L) - 8 F 10.0

DHP(I,L) Head (ft) associated with L^{th} pump rating curve; I index goes from 1 to 8; head starts at smallest and proceeds to greatest; negative head may be specified. Omit this card if NQLP(K)=0.

(45) OP(I,L) - 8 F 10.0

OP(I,L) Pump discharge (cfs) associated with L^{th} pump rating curve; I index goes from 1 to 8; each value is associated with its corresponding DHP(I,L) value. Omit this card if NQLP(K)=0.

Note Repeat card no. 43 to 45 as L index goes from 1 to NPM.

(46) LQX(K) - 8 I 10 Format

LQX(K) Number of cross-section immediately upstream of lateral inflow/outflow; K goes from 1 to LQ (card (16)). If LQX(K) is specified as a negative number, this indicates that the reach may have outflow via broad-crested weir flow.

(47) QL(L,K) - 8 F 10.0 Format

QL(L,K) Lateral inflow (cfs) for k^{th} lateral inflow point; L index goes from 1 to ITEH (card (2)); ordinates of lateral inflow hydrograph have same times as those of reservoir inflow hydrograph (QI(L)) on card (14)); K index goes from 1 to LQ.

If LQX(K) is negative, two values only are specified on card (47) according to a 2 F 10.2 format. The first (WELV(K)) is the crest elevation (msl) at which overflow occurs (this represents the average crest elevation along the reach). The second (CWR(K)) is the discharge coefficient ranging in value from 2.6 to 3.2 with 3.0 a most common value.

Note: Omit cards (46) and (47) if LQ=0 (on card no. 16).

(48) YD(I) - 8 F 10.0 Format

YD(I) — Initial water surface elevations (m.s.l.) along routing reach; this is used only if YDN=1.0; if YDN≠1.0, omit this card and program computes the initial water surface elevations.

(49) RH(K) - 8 F 10.0 Format

RH(K) — Elevation (m.s.l.) points on single value rating curve for downstream boundary, read in only if YDN (card no. 33) = 0.25; K index goes from 1 to maximum of 8.

(50) RQ(K) - 8 F 10.0 Format

RQ(K) — Discharge (cfs) associated with elevation points on single value rating curve for downstream boundary, read in only if YDN=0.25.

(51) STN(K) - 8 F 10.0 Format

STN(K) — Specified water surface elevation (m.s.l.) at downstream boundary such as a tide; K goes from 1 to ITEH, read in only if YDN=0.75.

(52) TTN(K) - 8 F 10.0 Format

TTN(K) — Time (hrs) associated with STN(K); K goes from 1 to ITEH, read in only if YDN=0.75.

(53) NSLI - I 10 Format

NSLI — Total no. of cross-sections (read-in) where landslide occurs; maximum no. allowed is 6; also maximum total cross-sections (including interpolated ones created by DXM values on card (31)) is limited to 31; omit if KSL=0 (card (2)).

(54) NXSLI(K), TSL, HSL(K), HSM(K), HSU(K), THKSL(K), ALPHA, POR - I 10, 7 F 10.2 Format

NXSLI(K)	Sequential number of cross-section where landslide occurs; K index goes from 1 to NSLI.
TSL	Time of duration for landslide (usually in the range of 15 seconds to a few minutes); unit must be in hrs.
HSL(K)	Elevation (ft above m.s.l.) of lowest portion of landslide mass; K goes from 1 to NSLI.
HSM(K)	Elevation (ft above m.s.l.) of middle portion of landslide mass--at this elevation, the landslide mass has the greatest thickness into the bank; K goes from 1 to NSLI.
HSU(K)	Elevation (ft above m.s.l.) of highest portion of landslide mass, K goes from 1 to NSLI.
THKSL(K)	Greatest thickness (depth into the bank) in ft of the landslide mass at elevation HSM(K); K goes from 1 to NSLI.
ALPHA	Angle of repose that deposited material from the landslide assumes in the bottom of the reservoir, in degrees.
POR	Porosity of landslide material, decimal fraction.

Note: Omit cards (53) and (54) if KSL=0.

Note: Card (54) is repeated for each K as it goes from 1 to NSLI.

(55) ICG(K) - 8 I 10 Format

ICG(K)	Parameter indicating if a dam has time-dependent gate flow; if yes, ICG(K)=1; if no, ICG(K)=0; K goes from 1 to M, where M=MULDAM if MULDAM≥1 and M=1 if MULDAM=0.

(56) CGCG(L,K) - 8 F 10.0 Format

CGCG(L,K)	Spillway gate coefficient equal to area of gates (opened at time TCG(L,K)) x coefficient of discharge; L goes from 1 to KCG (see card 16); and K goes from 1 to the total number of dams having time-dependent gate control.

(57) GBL(L,K) - 8 F 10.0 Format

GBL(L,K)	Distance (ft) from bottom of gate to gate sill (HGT-card(9)); This distance is time dependent and is associated with the time array TCG(L,K); L and K index are same as described on card (56).

(58) TCG(L,K) - 8 F 10.0 Format

TCG(L,K)	Time (hrs) associated with CGCG(L,K); L goes from 1 to KCG; and K goes from 1 to the total number of dams having time-dependent gate control.

Note: Omit cards (55), (56, (57), and (58) if KCG=0 (on card no. 16).

(59) Z, YBMIN, BB, TFH - 4 F 10.0 Format

Z	Side slope (1:vertical to z:horizontal) of breach of downstream dam.
YBMIN	Lowest elevation (ft) that bottom of breach reaches; elevation is referenced to m.s.l. datum.
BB	Width (ft) of base of breach of downstream dam.
TFH	Time (hr) from beginning of breach formation of downstream dam until it reaches its maximum size.

(60) HF, HD, HSP, HGT, CS, CG, CDO, QT - 8 F 10.0 Format

HF	Elevation (ft) of water when failure of downstream dam commences; elevation is referenced to m.s.l. datum.
HD	Elevation (ft) of top of downstream dam; elevation is referenced to m.s.l. datum.
HSP	Elevation (ft) of uncontrolled spillway crest; elevation is referenced to m.s.l. datum.
HGT	Elevation (ft) of center of gate openings; elevation is referenced to m.s.l. datum.
CS	Discharge coefficient for uncontrolled spillway; it is equal to the coefficient of discharge (2.6-3.2) times the length (ft) of the spillway.
CG	Discharge coefficient for gate flow; it is equal to the coefficient of discharge (0.10-0.80) times the area of gates.
CDO	Discharge coefficient for uncontrolled weir flow over the top of the downstream dam; it is equal to the coefficient of discharge (2.6-3.2) times the length of the downstream dam crest (ft) less the length of the uncontrolled spillway and gates.

QT — Discharges (cfs) through turbines; this flow is assumed constant from start of computations until the downstream dam is completely breached; thereafter QT is assumed to be zero.

(61) QSPILL(K,1) - 8 F 10.0 Format

QSPILL(K,1) — Flow (cfs) of spillway or gate rating curve; k goes from 1 to maximum of 8.

(62) HEAD(K,1) - 8 F 10.0 Format

HEAD(K,1) — Head (ft) above spillway crest or gate center; head is associated with spillway flow or gate flow in rating curve.

Note: Cards (61) and (62) are read-in only if either HSP is non-zero and CS is zero or HGT is non-zero and CG is zero. This option allows a rating curve to be used for either the uncontrolled spillway or submerged gate rather than an equation for each using a constant discharge coefficient as in Eq. (17).

(63) UPSH, SOM, CMN - 3 F 10.0 Format

UPSH — Dummy variable, leave blank.
SOM — Slope of downstream channel (ft/mi) for first few miles below dam.
CMN — Average Manning's n for downstream channel for first few miles below dam.

Note: Cards (59-63) are omitted if KUI=0 and MULDAM=0 or if KKN=9.

Note: If KUI=1 and dynamic routing is used for the reservoir routing procedure, cards (6) and (7) are omitted and cards (8)-(58) and (51) apply to the reservoir characteristics. Then, cards (16)-(58) are read in again; this time they apply to the downstream channel and valley.

Note: If KKN=9, only a downstream routing is used to route a read-in hydrograph (cards (12)-(15)). Also, cards (16)-(25) and (28)-(58) are required.

Note: The program has the capability of simulating a total of 12 different cases. These are outlined as follows:

Option 1: Reservoir storage routing to compute outflow hydrograph from reservoir with subcritical dynamic routing of outflow hydrograph through entire length of downstream valley--KUI=0, KKN=1, KSUPC=0, MULDAM=0.
Input data cards--1-4, 6-58.

Option 2: Reservoir storage routing to compute outflow hydrograph from reservoir with supercritical dynamic routing of outflow hydrograph through entire length of downstream valley--KUI=0, KKN=1, KSUPC=1, MULDAM=0.
Input data cards--1-4, 6-58.

Option 3: Reservoir storage routing to compute outflow hydrograph from reservoir with supercritical dynamic routing of outflow hydrograph through upstream portion of downstream valley and subcritical dynamic routing through downstream portion of downstream valley--KUI=0, KKN=2, KSUPC=1, MULDAM=0.
Input data cards--1-4, 6-52, 16-58.

Option 4: Same as Option 1 except reservoir dynamic routing to compute outflow hydrograph from reservoir--KUI=1, KKN=2, KSUPC=0, MULDAM=0.
Input data cards--1-4, 8-58, 63, 16-52.

Option 5: Same as Option 2 except reservoir dynamic routing to compute outflow hydrograph from reservoir--KUI=1, KKN=2, KSUPC=1, MULDAM=0.
Input data cards--1-4, 8-58, 63, 16-52

Option 6: Same as Option 3 except reservoir dynamic routing to compute outflow hydrograph from reservoir--KUI=1, KKN=3, KSUPC=1, MULDAM=0.
Input data cards--1-4, 8-58, 63, 16-52, 16-52.

Option 7: Subcritical dynamic routing of input hydrograph through a channel-valley--KUI=0, KKN=9, KSUPC=0, MULDAM=0.
Input data cards--1-4, 12-52.

Option 8: Supercritical dynamic routing of input hydrograph through a channel-valley--KUI=0, KKN=9, KSUPC=1, MULDAM=0.
Input data cards--1-4, 12-52.

Option 9: "Sequential Method" Reservoir storage routing to compute outflow hydrograph from reservoir with subcritical dynamic routing of outflow hydrograph through downstream channel-reservoir having a dam which may fail--KUI=0, KKN=2, KSUPC=0, MULDAM=1.
Input data cards--1-4, 6-63, 16-63, ... 16-52.

Option 10: "Sequential Method" Reservoir dynamic routing to compute outflow hydrograph from reservoir with subcritical dynamic routing of outflow hydrograph through downstream channel-reservoir having a dam which may fail--KUI=1, KKN=3, KSUPC=0, MULDAM=1.
Input data cards--1-4, 8-58, 63, 16-63, ... 16-52.

Option 11: Simultaneous Method" Simultaneous computation method for single dam or bridge (structure) using dynamic routing in the reach upstream of the structure and downstream of the structure with special internal boundary conditions for flow thru the structure--KUI=1, KKN=1, MULDAM=1, KSUPC=0.
Input data cards--1-5, 8-11, 12-58. See note on page A-21 for input variables for bridge and embankment.

Option 12: Simultaneous Method" Simultaneous computation method for multiple dams and/or bridges (structures) using dynamic routing for all reaches with special internal boundary conditions for flow thru each structure--KUI=1, KKN=1, MULDAM=no. of dams and/or bridges, KSUPC=0.
Input data cards--1-5, 8-11, 8-11, 8-11, ... 12-58. See note on page A-21 for input variables and embankments.

5.0 INPUT DATA PREPARATION FOR EXAMPLE PROBLEM

A typical example of preparing data for DAMBRK programme is presented herein for simulating the Machhu-II dam failure which occurred in Gujarat on 11th August 1979. The input is prepared for executing option-1 of the programme. This option envisages reservoir storage routing to compute outflow hydrograph from reservoir with supercritical dynamic routing of outflow hydrograph through entire length of downstream valley with the following considerations:

1. Reservoir routing for determining outflow hydrograph (KUI=0)
2. Subcritical flow consideration in the entire down stream channel valley reach (KSUPC =0 and KKN=1)
3. There is no dam(s) existing below the dam under consideration (MULDAM =0)

The serial number of input cards required for this option are 1-4 and 6-58. The description of each of the data card used in the input data preparation is given herein. However, the manner in which each individual variable value has been arrived for Machhu-II dam failure problem is not brought out in this technical note and presented in the case study report of Machhu-II dam failure simulation using DAMBRK programme.

INPUT DATA STRUCTURE PREPARED FOR
MACHHU-II DAM FAILURE PROBLEM

Input Card group No.		Card No.	Col.No.	Variable	Value
(1)	(TITLE CARD)	(i)	1-20	MDAM	MACHHU DAM-II
			21-40	MRVR	MACHHU RIVER
			41-60	MNAME	-
		(ii)	1-40	MESAGE	NATIONAL INSTITUTE OF HYDROLOGY
			41-72	MESAGE	ROORKEE-247667 (UP)
(2)	(INPUT CONTROL PROGRAMME CARD)		1-10	KKN	1
			11-20	KUI	0
			21-30	MULDAM	0
			31-40	KDMP	3
			41-50	ITEH	27
			51-60	NPRT	0
			61-70	KFLP	0
			71-80	KSL	0
(3)			- NOT USED -		
(4)			- NOT USED -		
(5)		NOT NECESSARY FOR THIS OPTION			
(6)	(RESERVOIR VOLUME CARD)	(i)	1-10	SA(1)	177915 (AC-ft)
			11-20	SA(2)	158402 (AC-ft)
			21-30	SA(3)	128318 (AC-ft)
			31-40	SA(4)	60026 (AC-ft)
			41-50	SA(5)	38092 (AC-ft)
			51-60	SA(6)	21359 (AC-ft)
			61-70	SA(7)	792 (AC-ft)
			71-80	SA(8)	0.0 (AC-ft)
(7)	(RESERVOIR ELEVATION CARD)	(i)	1-10	HSA(1)	198.50 ft
			11-20	HSA(2)	197.00 ft
			21-30	HSA(3)	194.00 ft
			31-40	HSA(4)	184.00 ft
			41-50	HSA(5)	178.00 ft
			51-60	HSA(6)	170.00 ft
			61-70	HSA(7)	155.00 ft
			71-80	HSA(8)	130.00 ft
(8)	(RESERVOIRS & BREACH PARAMETERS CARD)		1-10	RLM	4.30 miles
			11-20	YO	198.50 ft
			21-30	Z	0.03

		31-40	YBMIN	130.00 ft
		41-50	BB	1036.00 ft
		51-60	TFH	1.00 hr
		61-70	DATUM	130.00 ft
		71-80	VOL	1
(9)	(RESERVOIRS & BREACH PARAMETERS) (i)	1-10	HF	198.50 ft
		11-20	HD	197.00 ft
		21-30	HSP	168.00 ft
		31-40	HGT	0.00
		41-50	CS	0.00
		51-60	CG	0.00
		61-70	CDO	27055
		71-80	QT	0.00
(10)	(SPILLWAY RATING CURVE CARD) (i)	1-10	QSPILL(1,1)	229217 cfs
		11-20	QSPILL(2,1)	205069 cfs
		21-30	QSPILL(3,1)	184780 cfs
		31-40	QSPILL(4,1)	160690 cfs
		41-50	QSPILL(5,1)	103149 cfs
		51-60	QSPILL(6,1)	63751 cfs
		61-70	QSPILL(7,1)	17190 cfs
		71-80	QSPILL(8,1)	0 cfs
(11)	(i)	1-10	HEAD(1,1)	0.0 ft
		11-20	HEAD(2,1)	4.0 ft
		21-30	HEAD(3,1)	10.0 ft
		31-40	HEAD(4,1)	14.0 ft
		41-50	HEAD(5,1)	21.0 ft
		51-60	HEAD(6,1)	24.0 ft
		61-70	HEAD(7,1)	27.0 ft
		71-80	HEAD(8,1)	30.5 ft
(12)	(i)	1-10	DHF	2.00 hr
		11-20	TEH	52.00 hr
(13)	NOT NECESSARY AS VARIABLE ITEM (CARD 2) IS NON ZERO			
(14)	(i)	1-10	QI(1)	464000 cfs
		11-20	QI(2)	420000 cfs
		21-30	QI(3)	350000 cfs
		31-40	QI(4)	276000 cfs
		41-50	QI(5)	194000 cfs
		51-60	QI(6)	134000 cfs
		61-70	QI(7)	92000 cfs
		71-80	QI(8)	74500 cfs
	(ii)	1-10	QI(9)	58000 cfs
		11-20	QI(10)	42000 cfs
		21-30	QI(11)	30000 cfs
		31-40	QI(12)	20000 cfs
		41-50	QI(13)	10000 cfs

			51-60	QI(14)	4000 cfs
			61-70	QI(15)	2000 cfs
			71-80	QI(16)	2000 cfs
		(iii)	1-10	QI(17)	2000 cfs
			11-20	QI(18)	2000 cfs
			21-30	QI(19)	2000 cfs
			31-40	QI(20)	2000 cfs
			41-50	QI(21)	2000 cfs
			51-60	QI(22)	2000 cfs
			61-70	QI(23)	2000 cfs
			71-80	QI(24)	2000 cfs
		(iv)	1-10	QI(25)	2000 cfs
			11-20	QI(26)	2000 cfs
			21-30	QI(27)	2000 cfs
(15)	(INFLOWTIME CARD)	NOT NECESSARY AS DHF IS NON ZERO			
(16)	(RIVER REACH CROSS SECTIONAL PARAMETERS CARD)	(i)	1-10	NS	6
			11-20	NCS	8
			21-30	NTT	6
			31-40	JNK	4
			41-50	KSA	0
			51-60	KSUPC	0
			61-70	LQ	0
			71-80	KCG	0
(17)		(i)	1-10	NT(1)	1
			11-20	NT(2)	2
			21-30	NT(3)	3
			31-40	NT(4)	4
			41-50	NT(5)	5
			51-60	NT(6)	6
(18)	OMITTED				
(19)	OMITTED				
(20)	(CROSS-SECTIONAL VARIABLES)	(i)	1-10	XS(1)	0
			11-20	FSTG(1)	-
			21-30	XSL(1)	-
			31-40	XSR(1)	-
(21)	(ELEVATION CORRESPONDING TO TOP WIDTH CARD)	(i)	1-10	HS(1,1)	121.15 ft
			11-20	HS(2,1)	122.11 ft
			21-30	HS(3,1)	123.98 ft
			31-40	HS(4,1)	148.1 ft
			41-50	HS(5,1)	158.63 ft
			51-60	HS(6,1)	160.65 ft
			61-70	HS(7,1)	166.98 ft
			71-80	HS(8,1)	168.41 ft

(22)	(TOP WIDTH OF ACTIVE FLOW PORTION OF CHANNEL CROSS SECTION)	(i)	1-10	BS(1,1)	0.0
			11-20	BS(2,1)	459.32 ft
			21-30	BS(3,1)	615.16 ft
			31-40	BS(4,1)	1099.08 ft
			41-50	BS(5,1)	1476.4 ft
			51-60	BS(6,1)	3280.8 ft
			61-70	BS(7,1)	5905.00 ft
			71-80	BS(8,1)	6561. ft

(23) & (24) - CARD GROUP NOS. 23 AND 24 ARE OMITTED WHEN KFLP =0

(25)	(TOP WIDTH OF OFF CHANNEL STORAGE PORTION)	(i)	1-10	BSS(1,1)	0.0
			11-20	BSS(2,1)	0.0
			21-30	BSS(3,1)	0.0
			31-40	BSS(4,1)	0.0
			41-50	BSS(5,1)	1066.3
			51-60	BSS(6,1)	3445
			61-70	BSS(7,1)	2132.5
			71-80	BSS(8,1)	1804.5

CARD GROUP NOS. 20,21,22, AND 25 HAVE BEEN REPEATED FOR CROSS-SECTION NUMBERS 2,3 ,4,5 AND 6 . THE DATA INPUT FOR THESE CROSS-SECTIONS HAVE BEEN PRESENTED IN THE INPUT DATA LISTING

(26) & (27)- CARD GROUP NOS. 26 AND 27 ARE OMITTED WHEN KSA=0

(28)	(MANNING'S n CARD CORRESPONDING TO EACH ELEVATION OF A GIVEN REACH)	(i)	1-10	CM(1,1)	0.035
			11-20	CM(2,1)	0.030
			21-30	CM(3,1)	0.03
			31-40	CM(4,1)	0.03
			41-50	CM(4,1)	0.03
			51-60	CM(6,1)	0.03
			61-70	CM(7,1)	0.03
			71-80	CM(8,1)	0.03

CARD GROUP NO 28 IS REPEATED FOR OTHER FOUR REACHES AND THE DATA INPUT FOR THESE REACHES HAVE BEEN PRESENTED IN THE INPUT DATA LISTING

(29) & (30) - CARD GROUP NOS.29 AND 30 ARE NOT NEEDED WHEN KFLP = 0 (CARD GROUP 2)

(31)	(MINIMUM DISTANCE TO BE USED IN THE COMPUTATION WITHIN THE GIVEN REACH)	(i)	1-10	DXM(1)	0.5
			11-20	DXM(2)	0.5
			21-30	DXM(3)	0.5
			31-40	DXM(4)	0.5
			41-50	DXM(5)	0.5

(32)	(CONTRACTION-EXPANSION COEFFICIENT CARD)	(i)	1-10	FKC(1)	0.0
			11-20	FKC(2)	0.0
			21-30	FKC(3)	-0.5
			31-40	FKC(4)	-0.5
			41-50	FKC(5)	-0.5
(33)	(DOWNSTREAM FLOW PARAMETERS CARD)	(i)	1-10	QMAXD	0.0
			11-20	QLL	0.0
			21-30	DTHM	0.0
			31-40	VDN	0.0
			41-50	SOM	7.87
			51-60	THETA	0.0
			61-70	EPSY	0.0
			71-80	TFI	52.0 hr

(34) TO (58) - CARD GROUP NOS.34 TO 58 ARE NOT NEEDED BECAUSE OF VARIOUS OPTIONS CONSIDERED UNTIL CARD GROUP NO.33.

INPUT FILE FOR EXAMPLE DAM-BREAK ANALYSIS

```
MACHHU DAM-II      MACHHU RIVER
NATIONAL INSTITUTE OF HYDROLOGY                    ROORKEE-247667(U.P)
     1          0          0          3         27
177915     158402     128318      60026      38092      21359       7926         0.
 198.5        197        194        184        178        170        155        130
   4.3      198.5       .027       130.      1036.        1.0       130.         1.
 198.5      197.0       168.         0.         0.         0.      27055.         0.
    0.      17190.     63751.     103149.    160690.    184780.    205069.    229217.
    0.        4.0        10.        14.        21.        24.        27.        30.5
    2.        52.
464000.     420000     350000     276000     194000     134000      92000      74500
 58000.      42000      30000      20000      10000       4000       2000       2000
  2000.       2000       2000       2000       2000       2000       2000       2000
  2000.       2000       2000
     6          8          6          4          0          0          0          0
     1          2          3          4          5          6
    0.
121.15     122.11     123.98     148.18     158.63     160.65     166.98     168.41
    0.     459.32     615.16    1099.08    1476.40    3280.80    5905.50    6561.70
    0.         0.         0.         0.    1066.30    3445.00    2132.50    1804.50
 5.813
 86.81      94.78     105.07     110.27     123.85     125.87     127.18     131.00
    0.     738.19    1269.69    1443.60    1919.30    2263.80    2657.50    2706.70
    0.         0.         0.         0.         0.         0.         0.    9842.5
 10.81
 44.59      47.08      66.72      88.11      88.78      90.94      93.34     101.12
    0.     492.13     853.02    1837.27    2575.50    2625.00    4265.10    4921.30
    0.         0.       98.4     574.15      531.5      623.40     1148.3    7053.8
 15.81
 27.73      34.32      37.57      56.78      68.36      71.92      72.92      77.00
    0.     354.33     534.78     918.64    2378.60    3608.90    6889.80    9843.00
    0.         0.         0.         0.         0.      3412.      5413.      9022.
 20.69
 17.69      17.88      22.89      32.48      40.78      45.15      48.35      52.97
    0.     170.60     354.30     659.40    1141.70    2625.00    7874.00   19685.0
    0.         0.         0.         0.         0.       610.      1509.      2625.
 24.63
  2.91      15.59      26.05      30.73      32.48      32.81      34.45      36.09
    0.     262.47     278.90     820.20   11811.00    22966.0    26247.0    29528.0
    0.         0.         0.         0.         0.         0.         0.         0.
  .035       .035       .035       .035       .035       .035       .035       .035
  .035       .035       .035       .035       .035       .035       .035       .035
  .035       .035       .035       .035       .035       .035       .035       .035
  .03        .03        .03        .03        .03        .03        .03        .03
  .03        .03        .03        .03        .03        .03        .03        .03
  0.5        0.5        0.5        0.5        0.5
  0.0        0.0       -0.5       -0.5       -0.5
  0.0        0.0        0.0        0.0       7.87        0.0        0.0         0.
```

REFERENCES

1. Fread, D.L. (1977), 'DAMBRK: The NWS Dam-break Flood Forecasting Model', Office of Hydrology, National Weather Service, Silver Spring, Maryland.

2. Fread, D.L. (1984),'DAMBRK : The NWS Dam-break Flood Forecasting Model', Office of Hydrology, National Weather Service, Silver Spring, Maryland.

3. The Hydrologic Engineering Center,(1984), 'DAMBRK: The NWS Dam-break Flood Forecasting Model', Users Manual (Preliminary), Davis, California.

4. Ritter, A. (1982),'The propagation of Water Waves', Ver. Deutsch Ingenieure Zeitschr (Berlin), 36, Pt.2, No.33, pp.947-954.

APPENDIX-I

DAMBRK MODEL DESCRIPTION

1.0 INTRODUCTION

The DAMBRK model attempts to represent the current state-of-the-art in understanding of dam failures and the utilization of hydrodynamic theory to predict the dam-break wave formation and downstream progression. The model has wide applicability; it can function with various levels of input data ranging from rough estimates to complete data specification; the required data is readily accessible; and it is economically feasible to use, i.e., it requires a minimal computation effort on large computing facilities.

The model consists of three functional parts, namely: (1) description of the dam failure mode, i.e., the temporal and geometrical description of the breach; (2) computation of the time history (hydrograph) of the outflow through the breach as affected by the breach description, reservoir inflow, reservoir storage characteristics, spillway outflows, and downstream tailwater elevations; and (3) routing of the outflow hydrograph through the downstream valley in order to determine the changes in the hydrograph due to valley storage, frictional resistance, downstream bridges or dams, and to determine the resulting water surface elevations (stages) and flood-wave travel times.

DAMBRK is an expanded version of a practical operational model first presented in 1977 by (Fread, 1977). That model was based on previous work on modeling breached dams (Fread and Harbaugh, 1973) and routing of flood waves (Fread, 1974, 1976). There have been a number of other operational dam-break models that have appeared recently in the literature, e.g., Price, et al. (1977), Gundlach and Thomas (1977), Thomas (1977), Keefer and Simons (1977), Chen and Druffel (1977) Balloffet, et al. (1974), Balloffet (1977), Brown and Rogers (1977), Rajar (1978), Brevard and Theurer (1979). DAMBRK differs from each of these models in the treatment of the breach formation, the outflow hydrograph generation, and the downstream flood routing.

1.1 Breach Description

The breach is the opening formed in the dam as it fails. The actual failure mechanics are not well understood for either earthen or concrete dams. In previous attempts to predict downstream flooding due to dam failures, it was usually assumed that the dam failed completely and instantaneously. Investigators of dam-break flood waves such as

Ritter (1892), Schocklitsch (1917), Re (1946), Dressler (1954), Stoker (1957), Su and Barnes (1969), and Sakkas and Strelkoff (1973) assumed the breach encompasses the entire dam and that it occurs instantaneously. Others, such as Schocklitsch (1917) and Army Corps of Engineers (1960), have recognized the need to assume partial rather than complete breaches; however, they assumed the breach occurred instantaneously. The assumptions of instantaneous and complete breaches were used for reasons of convenience when applying certain mathematical techniques for analyzing dam-break flood waves. These assumptions are somewhat appropriate for concrete arch-type dams, but they are not appropriate for earthen dams and concrete gravity-type dams.

Earthen dams which exceedingly outnumber all other types of dams do not tend to completely fail, nor do they fail instantaneously. The fully formed breach in earthen dams tends to have an average width ($\bar{b}$) in the range ($h_d < \bar{b} < 3h_d$) where h_d is the height of the dam. The middle portion of this range for $\bar{b}$ is supported by the summary report of Johnson and Illes (1976). Breach widths for earthen dams are therefore usually much less than the total length of the dam as measured across the valley. Also, the breach requires a finite interval of time for its formation through erosion of the dam materials by the escaping water. Total time of failure may be in the range of a few minutes to a few hours, depending on the height of the dam, the type of materials used in construction, the extent of compaction of the materials, and the extent (magnitude and duration) of the overtopping flow of the escaping water. Piping failures occur when initial breach formation takes place at some point below the top of the dam due to erosion of an internal channel through the dam by escaping water. As the erosion proceeds, a larger and larger opening is formed; this is eventually hastened by caving-in of the top portion of the dam.

Concrete gravity dams also tend to have a partial breach as one or more monolith sections formed during the construction of the dam are forced apart by the escaping water. The time for breach formation is in the range of a few minutes.

Poorly constructed earthen dams and coal-waste slag piles which impound water tend to fail within a few minutes, and have average breach widths in the upper range or even greater than those for the earthen dams mentioned above.

Cristofano (1965) attempted to model the partial, time-dependent breach formation in earthen dams; however, this procedure requires critical assumptions and specification of unknown critical parameter values. Also, Harris and Wagner (1967) used a sediment transport relation to determine the time for breach formation, but this procedure requires specification of breach size and shape in addition to two critical parameters for the sediment transport relation.

For reasons of simplicity, generality, wide applicability, and the uncertainty in the actual failure mechanism, the NWS DAMBRK model allows the forecaster to input the failure time interval (τ) and the terminal

size and shape of the breach (Fread and Harbaugh, 1973). The shape is specified by a parameter (z) identifying the side slope of the breach, i.e., 1 vertical: z horizontal slope. The range of z values is: $0 \leq z \leq 2$. Rectangular triangular, or trapezoidal shapes may be specified in this way. For example, Z=0 and b>0 produces a trapezoidal shape. The final breach size is controlled by the z parameter and another parameter (b) which is the terminal width of the bottom of the breach. As shown in Fig. 1, the model assumes the breach bottom width starts at a point and enlarges at a linear rate over the failure time interval (τ) until the terminal width is attained and the breach bottom has eroded to the elevation h_{bm} which is usually, but not necessarily, the bottom of the reservoir or outlet channel bottom. If τ is less than 10 minutes, the width of the breach bottom starts at a value of b rather than at a point. This represents more of a collapse failure than an erosion failure.

During the simulation of a dam failure, the actual breach formation commences when the reservoir water surface elevation (h) exceeds a specified value, h_f. This feature permits the simulation of an overtopping of a dam in which the breach does not form until a sufficient amount of water is flowing over the crest of the dam. A piping failure may be simulated when h_f is specified less than the height of the dam, h_d.

Selection of breach parameters before a breach forms, or in the absence of observations, introduces a varying degree of uncertainty in the model results; however, errors in the breach description and thence in the resulting time rate of volume outflow are rapidly damped-out as the flood wave advances downstream. For conservative forecasts which err on the side of larger flood waves, values for b and z should produce an average breach width ($\bar{b}$) in the uppermost range for a certain type of dam. Failure time (τ) should be selected in the lower range to produce a maximum outflow. Of course, observational estimates of $\bar{b}$ and τ should be used when available to update forecasts when response time is sufficient as in the case of forecast points several miles downstream of

the structure. Flood wave travel rates are often in the range of 2-10 miles per hour. Accordingly, response times for some downstream forecast points may therefore be sufficient for updated forecasts to be issued.

1.2 Reservoir Outflow Hydrograph

The total reservoir outflow consists of broad-crested weir flow through the breach and flow through any spillway outlets, i.e.,

$$Q = Q_b + Q_s \tag{1}$$

The breach outflow (Q_b) is computed as:

$$Q_b = c_1(h-h_b)^{1.5} + c_2(h-h_b)^{2.5} \tag{2}$$

where:

$$c_1 = 3.1\ b_1\ c_v\ k_s \tag{3}$$

$$c_2 = 2.45\ z\ c_v\ k_s \tag{4}$$

$$h_b = h_d - (h_d - h_{bm})\ \frac{t_b}{\tau} \qquad \text{if} \qquad t_b \leq \tau \tag{5}$$

$$h_b = h_{bm} \qquad \text{if} \qquad t_b > \tau \tag{6}$$

$$b_1 = b\ t_b/\tau \qquad \text{if} \qquad t_b \leq \tau \tag{7}$$

$$c_v = 1.0 + 0.023\ Q^2/[B_d^2\ (h-h_{bm})^2\ (h-h_b)] \tag{8}$$

$$k_s = 1.0 \qquad \text{if} \qquad \frac{h_t-h_b}{h-h_b} \leq 0.67 \tag{9}$$

otherwise:

$$k_s = 1.0 - 27.8\ \left[\frac{h_t-h_b}{h-h_b} - 0.67\right]^3 \tag{10}$$

in which h_b is the elevation of the breach bottom, h is the reservoir water surface elevation, b_1 is the instantaneous breach bottom width, t_b is time interval since breach started forming, c_v is correction for velocity of approach (Brater, 1959), Q is the total outflow from the reservoir, B_d is width of the reservoir at the dam, k_s is the submergence correction for tailwater effects on weir outflow (Benard, 1954),

and h_t is the tailwater elevation (water surface elevation immediately downstream of dam).

The tailwater elevation (h_t) is computed from Manning's equation, i.e.,

$$Q = \frac{1.49}{n} S^{1/2} \frac{A^{5/3}}{B^{2/3}} \tag{11}$$

in which n is the Manning roughness coefficient, A is the cross-sectional area of flow, B is the top width of the wetted cross-sectional area, and S is the energy slope. Each term in equation 11 applies to a representative channel reach immediately downstream of the dam. The S parameter can be specified by the user; it does not change with time; if it is not specified, the model uses the channel bottom slope of the first third of the downstream valley reach. Since A and B are functions of h_t and Q is the total discharge given by equation 1, and 11 provides a sufficiently accurate value for h_t if there are no backwater effects immediately below the dam due to downstream constrictions, dams, bridges, or significant tributary inflows. When these affect the tailwater, equation 11 is not used and another procedure, referred to herein as the "simultaneous method," which is described in a following section on multiple dams and bridges is used.

If the breach is formed by piping, equations 2-9 are replaced by the following orifice flow equation:

$$Q_b = 4.8 A_p (h-\bar{h})^{1/2} \tag{12}$$

where:

$$A_p = [2b_1+4z(h_f-h_b)] (h_f-h_b) \tag{13}$$

$$\bar{h} = h_t \qquad \text{if} \qquad h_t < 2h_f - h_b \tag{14}$$

$$\bar{h} = h_t \qquad \text{if} \qquad h_t > 2h_f - h_b \tag{15}$$

and h_d is replaced by h_f in equation 5 to compute h_b.

However, if $\bar{h} = h_f$ and

$$h - h_b < 2.2(h_f-h_b) \tag{16}$$

the flow ceases to be orifice flow and the broad-crested weir flow, equation 2, is used.

The spillway outflow (Q_s) is computed as:

$$Q_s = c_s L_s (h-h_s)^{1.5} + c_g A_g (h-h_g)^{0.5} + c_d L_d (h-h_d)^{1.5} + Q_t \qquad (17)$$

in which c_s is the uncontrolled spillway discharge coefficient, h_s is the uncontrolled spillway crest elevation, c_g is the gated spillway discharge coefficient, h_g is the center-line elevation of the gated spillway, c_d is the discharge coefficient for flow over the crest of the dam L_s is the spillway length, A_g is the gate flow area, L_d is the length of the dam crest less L_s, and Q_t is a constant outflow term which is head independent. The uncontrolled spillway flow or the gated spillway flow can also be represented as a table of head-discharge values. The gate flow may also be specified as a function of time.

The total outflow is a function of the water surface elevation (h). Depletion of the reservoir storage volume by the outflow causes a decrease in h which then causes a decrease in Q. However, any inflow to the reservoir tends to increase h and Q. In order to determine the total outflow (Q) as function of time, the simultaneous effects of reservoir storage characteristics and reservoir inflow require the use of a reservoir routing technique. DAMBRK utilizes a hydrologic storage routing technique based on the law of conservation of mass, i.e.,

$$I - Q = dS/dt \qquad (18)$$

in which I is the reservoir inflow, Q is the total reservoir outflow, and dS/dt is the time rate of change of reservoir storage volume. Eq. (18) may be expressed in finite difference form as:

$$(I+I')/2 - (Q+Q')/2 = \Delta S/\Delta t \qquad (19)$$

in which the prime (') superscript denotes values at the time $t-\Delta t$ and the Δ approximates the differential. The term ΔS may be expressed as:

$$\Delta S = (A_s+A_s') (h-h')/2 \qquad (20)$$

in which A_s is the reservoir surface area coincident with the elevation (h).

Combining equations(1), (2), (17), (19) and (20) result in the following expression:

$$(A_s+A_s') (h-h')/\Delta t + c_1(h-h_b)^{1.5} + c_2(h-h_b)^{2.5} + c_s(h-h_b)^{1.5}$$

$$+ c_g(h-h_g)^{0.5} + c_d(h-h_d)^{1.5} + Q_t + Q' - I - I' = 0 \qquad (21)$$

Since A_s is a function of h and all other terms except h are known, Eq. (21) can be solved for the unknown h using Newton-Raphson iteration.

Having obtained h, usually within two or three iterations, equation 2 and (17) can be used to obtain the total outflow (Q) at time (t). In this way the outflow hydrograph Q(t) can be developed for each time (t) as t goes from zero to some terminating value (t_e) sufficiently large for the reservoir to be drained. In equation 21 the time step (Δt) is chosen sufficiently small to incur minimal numerical integration error. This value is preset in the model to $\tau/50$.

The hydrologic storage routing technique, equation 18, implies that the water surface elevation within the reservoir is level. This assumption is quite adequate for gradually occurring breaches with no substantial reservoir inflow hydrographs. However, when 1) the breach is specified to form almost instantaneously so as to produce a negative wa e within the reservoir, and/or 2) the reservoir inflow hydrograph is significant enough to produce a positive wave progressing through the reservoir, a routing technique which simulates the negative and/or positive wave(s) occurring within the reservoir could be used for greater accuracy in computing the reservoir outflow through the breach and/or spillways. Such a technique is referred to as dynamic routing. Since this technique is used for routing the dam-break flood wave through the downstream valley, the application of it in lieu of reservoir storage routing will be presented after the downstream routing technique is presented.

1.3 Downstream Routing

After computing the hydrograph of the reservoir outflow, the extent of and time of occurrence of flooding in the downstream valley is determined by routing the outflow hydrograph through the valley. The hydrograph is modified (attenuated, lagged, and distorted) as it is routed through the valley due to the effects of valley storage, frictional resistance to flow, flood wave acceleration components, and downstream obstructions and/or flow control structures. Modifications to the dam-break flood wave are manifested as attenuation of the flood peak elevation, spreading-out or dispersion of the flood wave volume, and changes in the celerity (translation speed) or travel time of the flood wave. If the downstream valley contains significant storage volume such as a wide flood plain, the flood wave can be extensively attenuated and its time of travel greatly increased. Even when the downstream valley approaches that of a uniform rectangular-shaped section, there is appreciable attenuation of the flood peak and reduction in the wave celerity as the wave progresses through the valley.

A distinguishing feature of dam-break waves is the great magnitude of the peak discharge when compared to runoff-generated flood waves having occurred in the past in the same valley. The dam-break flood is usually many times greater than the runoff flood of record. The above-record discharges make it necessary to extrapolate certain coefficients used in various flood routing techniques and make it impossible to fully calibrate the routing technique.

Another distinguishing characteristic of dam-break floods is the very short duration time, and particularly the extremely short time from beginning of rise until the occurrence of the peak. The time to peak is in almost all instances synonymous with the breach formation time (τ) and therefore is in the range of a few minutes to a few hours. This feature, coupled with the great magnitude of the peak discharge, causes the dam-break flood wave to have acceleration components of a far greater significance than those associated with a runoff-generated flood wave.

There are two basic types of flood routing methods, the hydrologic and the hydraulic methods. The hydrologic methods are more of an approximate analysis of the progression of a flood wave through a river reach than are the hydraulic methods. The hydrologic methods are used for reasons of convenience and economy. They are most appropriate as far as accuracy is concerned when the flood wave is not rapidly varying, i.e., the flood wave acceleration effects are negligible compared to the effects of gravity and channel friction. Also, they are best used when the flood waves are very similar in shape and magnitude to previous flood waves for which stage and discharge observations are available for calibrating the hydrologic routing parameters (coefficients).

For routing dam-break flood waves, a particular hydraulic method known as the dynamic wave method is chosen. This choice is based on its ability to provide more accuracy in simulating the dam-break flood wave than that provided by the hydrologic methods, as well as other hydraulic methods such as the kinematic wave and diffusion wave methods. Of the many available hydrologic and hydraulic routing techniques, only the dynamic wave method accounts for the acceleration effects associated with the dam-break waves and the influence of downstream unsteady backwater effects produced by channel constrictions, dams, bridge-road embankments, and tributary inflows. Also, the dynamic wave method can be used economically, i.e., the computational costs can be made insignificant if advantages of certain numerical solution techniques are utilized.

The dynamic wave method based on the complete equations of unsteady flow is used to route the dam-break flood hydrograph through the downstream valley. This method is derived from the original equations developed by Barre De Saint-Venant (1871). The only coefficient that must be extrapolated beyond the range of past experience is the coefficient of flow resistance. It so happens that this is usually not a sensitive parameter in effecting the modifications of the flood wave due to its progression through the downstream valley. The applicability of Saint-Venant equations to simulate abrupt waves such as the dam-break wave has been demonstrated by Terzidis and Strelkoff (1970) and by Martin and Zovne (1971) who used a "through computation" method which ignores the presence of shock waves. DAMBRK uses the "through computation" method as opposed to isolating a single shock wave should it occur, and then applying the shock equations to it and using the Saint-Venant equations for all other portions of the flow.

The Saint-Venant unsteady flow equations consist of a conservation of mass equation, i.e.,

$$\frac{\partial Q}{\partial x} + \frac{\partial (A+A_o)}{\partial t} - q = 0 \qquad (22)$$

and a conservation of momentum equation, i.e.,

$$\frac{\partial Q}{\partial x} + \frac{\partial (Q^2/A)}{\partial x} + gA\left(\frac{\partial h}{\partial x} + S_f + S_e\right) = 0 \qquad (23)$$

where A is the active cross-sectional area of flow, A_o is the inactive (off-channel storage) cross-sectional area, x is the longitudinal distance along the channel (valley), t is the time, q is the lateral inflow or outflow per linear distance along the channel (inflow is positive and outflow is negative in sign), g is the acceleration due to gravity, S_f is the friction slope, and S_e is the expansion-contraction slope. The friction slope is evaluated from Manning's equation for uniform, steady flow, i.e.,

$$S_f = \frac{n^2 |Q| Q}{2.21\ A^2\ R^{4/3}} \qquad (24)$$

in which n is the Manning coefficient of frictional resistance and R is the hydraulic radius defined as A/B where B is the top width of the active cross-sectional area. The term (S_e) is defined as follows:

$$S_e = \frac{k\ \Delta(Q/A)^2}{2g\ \Delta x} \qquad (25)$$

in which k (Morris and Wiggert, 1972) is the expansion-contraction coefficient varying from 0.0 to ±1.0 (+ if contraction, - if expansion), and $\Delta(Q/A)^2$ is the difference in the term $(Q/A)^2$ at two adjacent cross-sections separated by a distance Δx. L is the momentum effect of lateral flow assumed herein to enter or exit perpendicular to the direction of the main flow. This term has the following form: 1) lateral inflow, L = 0; 2) seepage lateral outflow, L = -0.5qQ/A; and 3) bulk lateral outflow, L = -qQ/A.

Equations 22 - 23 were modified by Fread (1975, 1976) and Smith (1978) to better account for the differences in flood wave properties for flow occurring simultaneously in the river channel and the overbank flood plain of the downstream valley. As modified, equation 22-(23) become:

$$\frac{\partial (K_c Q)}{\partial x_c} + \frac{\partial (K_\ell Q)}{\partial x_\ell} + \frac{\partial (K_r Q)}{\partial x_r} + \frac{\partial A}{\partial t} - q = 0 \qquad (26)$$

$$\frac{\partial Q}{\partial t} + \frac{\partial(K_c^2 Q^2/A_c)}{\partial x_c} + \frac{\partial(K_\ell^2 Q^2/A_\ell)}{\partial x_\ell} + \frac{\partial(K_r^2 Q^2/A_r)}{\partial x_r} + gA_c \left[\frac{\partial h}{\partial x_c} + S_{fc} + S_e\right] + gA_\ell \left[\frac{\partial h}{\partial x_\ell} + S_{f\ell}\right] + gA_r \left[\frac{\partial h}{\partial x_r} + S_{fr}\right] = 0 \quad (27)$$

in which the subscripts (c), (ℓ), and (r) represent the channel, left flood-plain, and right flood-plain sections, respectively. The parameters (K_c, K_ℓ, K_r) proportion the total flow (Q) into channel flow, left flood-plain flow, and right flood-plain flow, respectively. These are defined as follows:

$$K_c = \frac{1}{1+k_\ell+k_r} \quad (28)$$

$$K_\ell = \frac{k_\ell}{1+k_\ell+k_r} \quad (29)$$

$$K_r = \frac{k_r}{1+k_\ell+k_r} \quad (30)$$

in which

$$k_\ell = \frac{Q_\ell}{Q_c} = \frac{n_c}{n_\ell}\frac{A_\ell}{A_c}\left[\frac{R_\ell}{R_c}\right]^{2/3}\left[\frac{\Delta x_c}{\Delta x_\ell}\right]^{1/2} \quad (31)$$

$$k_r = \frac{Q_r}{Q_c} = \frac{n_c}{n_r}\frac{A_r}{A_c}\left[\frac{R_r}{R_c}\right]^{1/2}\left[\frac{\Delta x_c}{\Delta x_r}\right]^{1/2} \quad (32)$$

Equations 31-32 represent the ratio of flow in the channel section to flow in the left and right flood-plain (overbank) sections, where the flows are expressed in terms of the Manning equation in which the energy slope is approximated by the water surface slope ($\Delta h/\Delta x$).

The friction slope terms in equation 27 are given by the following:

$$S_{fc} = \frac{n_c^2 |K_c Q| K_c Q}{2.21\, A_c^2 R_c^{4/3}} \quad (33)$$

$$S_{f\ell} = \frac{n_\ell^2 |K_\ell Q| K_\ell Q}{2.21\, A_\ell^2 R_\ell^{4/3}} \quad (34)$$

$$S_{fr} = \frac{n_r^2 |K_r Q| K_r Q}{2.21\, A_r^2 R_r^{4/3}} \quad (35)$$

In equation 26 the term A is the total cross-sectional area, i.e.,

$$A = A_c + A_\ell + A_r + A_o \tag{36}$$

where A_o is the off-channel storage (inactive) area.

Equations (22)-(23) and (26)-(27) constitute a system of partial differential equations of the hyperbolic type. They contain two independent variables, x and t, and two dependent variables, h and Q; the remaining terms are either functions of x, t, h, and/or Q, or they are constants. These equations are not amenable to analytical solutions except in cases where the channel geometry and boundary conditions are uncomplicated and the non-linear properties of the equations are either neglected or made linear. The equations may be solved numerically by performing two basic steps. First, the partial differential equations are represented by a corresponding set of finite difference algebraic equations; and second, the system of algebraic equations is solved in conformance with prescribed initial and boundary conditions.

Eqs. (22)-(23) and (26)-(27) can be solved by either explicit or implicit finite difference techniques (Liggett and Cunge, 1975). Explicit methods, although simpler in application, are restricted by mathematical stability considerations to very small computational time steps (on the order of a few minutes or even seconds). Such small time steps cause the explicit methods to be very inefficient in the use of computer time. Implicit finite difference techniques (Preissmann, 1961; Amein and Fang, 1970; Strelkoff, 1970), however, have no restrictions on the size of the time step due to mathematical stability; however, convergence considerations may require its size to be limited (Fread, 1974a).

Of the various implicit schemes that have been developed, the "weighted four-point" scheme first used by Preissmann(1961), and more recently by Chaudhry and Contractor (1973) and Fread (1974b, 1978) appears most advantageous since it can readily be used with unequal distance steps and its stability-convergence properties can be easily controlled. In the weighted four-point implicit finite difference scheme, the continuous x-t region in which solutions of h and Q are sought, is represented by a rectangular net of discrete points. The net points are determined by the intersection of lines drawn parallel to the x and t axes. Those parallel to the x axis represent time lines; they have a spacing of Δt, which also need not be constant. Each point in the rectangular network can be identified by a subscript (i) which designates the x position and a superscript (j) which designates the time line.

The time derivatives are approximated by a forward difference quotient centered between the i^{th} and i+1 points along the x axis, i.e.,

$$\frac{\partial K}{\partial t} = \frac{K_i^{j+1} + K_{i+1}^{j+1} - K_i^j - K_{i+1}^j}{2\,\Delta t_j} \tag{37}$$

where K represents any variable.

The spatial derivatives are approximated by a forward difference quotient positioned between two adjacent time lines according to weighting factors of Θ and $1-\Theta$, i.e.,

Page

i
$$\frac{\partial K}{\partial x} = \Theta \left[\frac{K_{i+1}^{j+1} - K_i^{j+1}}{\Delta x_i}\right] + (1-\Theta) \left[\frac{K_{i+1}^{j} - K_i^{j}}{\Delta x_i}\right] \qquad (38)$$

ii Variables other than derivatives are approximated at the time level where the spatial derivatives are evaluated by using the same weighting factors, i.e.,

iii
$$K = \Theta \left[\frac{K_i^{j+1} + K_{i+1}^{j+1}}{2}\right] + (1-\Theta) \left[\frac{K_i^{j} + K_{i+1}^{j}}{2}\right] \qquad (39)$$

1 A Θ weighting factor of 1.0 yields the fully implicit or backward difference scheme used by Baltzer and Lai (1968). A weighting factor of 0.5 yields the box scheme used by Amein and Fang (1970). The influence
4 of the Θ weighting factor on the accuracy of the computations was examined by Fread (1974a), who concluded that the accuracy decreases as Θ departs from 0.5 and approaches 1.0. This effect becomes more
7 pronounced as the magnitude of the computational time step increases. Usually, a weighting factor of 0.60 is used so as to minimize the loss of accuracy associated with greater values while avoiding the
17 possibility of a weak or pseudo instability noticed by Baltzer and Lai (1968), and Chaudhry and Contractor (1973); however, Θ may be specified other than 0.60 in the data input to the DAMBRK model.

37 When the finite difference operators defined by equation(37)-(39) are used to replace the derivatives and other variables inequation(22)-(23), the following weighted four-point implicit difference equations are
44 obtained:

$$\Theta \left[\frac{Q_{i+1}^{j+1} - Q_i^{j+1}}{\Delta x_i}\right] - \Theta\, q_i^{j+1} + (1-\Theta) \left[\frac{Q_{i+1}^{j} - Q_i^{j}}{\Delta x_i}\right] - (1-\Theta)\, q_i^{j}$$

$$+ \left[\frac{(A+A_o)_i^{j+1} + (A+A_o)_{i+1}^{j+1} - (A+A_o)_i^{j} - (A+A_o)_{i+1}^{j}}{2\Delta t_j}\right] = 0 \qquad (40)$$

$$\left(\frac{Q_i^{j+1} + Q_{i+1}^{j+1} - Q_i^{j} - Q_{i+1}^{j}}{2\Delta t_j}\right) + \Theta \left[\frac{(Q^2/A)_{i+1}^{j+1} - (Q^2/A)_i^{j+1}}{\Delta x_i} + g\, \bar{A}^{j+1}\right.$$

$$\left.\left(\frac{h_{i+1}^{j+1} - h_i^{j+1}}{\Delta x_i} + \bar{S}_f^{j+1} + S_{ce}^{j+1}\right)\right] + (1-\Theta) \left[\frac{(Q^2/A)_{i+1}^{j} - (Q^2/A)_i^{j}}{\Delta x_i}\right.$$

$$\left. + g\, \bar{A}^{j} \left(\frac{h_{i+1}^{j} - h_i^{j}}{\Delta x_i} + \bar{S}_f^{j} + S_{ce}^{j}\right)\right] = 0 \qquad (41)$$

where:

$$\bar{A} = (A_i + A_{i+1})/2 \tag{42}$$

$$\bar{S}_f = n^2 \bar{Q}|\bar{Q}|/(2.2\ \bar{A}^2\ \bar{R}^{4/3}) \tag{43}$$

$$\bar{Q} = (Q_i + Q_{i+1})/2 \tag{44}$$

$$\bar{R} = \bar{A}/\bar{B} \tag{45}$$

$$\bar{B} = (B_i + B_{i+1})/2 \tag{46}$$

The terms associated with the j^{th} time line are known from either the initial conditions or previous computations. The initial conditions refer to values of h and Q at each node along the x axis for the first time line (j=1).

Equations (40)-(41) cannot be solved in an explicit or direct manner for the unknowns since there are four unknowns and only two equations. However, if equation (40)-(41) are applied to each of the (N-1) rectangular grids between the upstream and downstream boundaries, a total of (2N-2) equations with 2N unknowns can be formulated. (N denotes the total number of nodes). Then, prescribed boundary conditions, one at the upstream boundary and one at the downstream boundary, provide the necessary two additional equations required for the system to be determinate. The resulting system of 2N non-linear equations with 2N unknowns is solved by a functional iterative procedure, the Newton-Raphson method (Amein and Fang, 1970).

Computations for the iterative solution of the non-linear system are begun by assigning trial values to the 2N unknowns. Substitution of the trial values into the system of non-linear equations yields a set of 2N residuals. The Newton-Raphson method provides a means for correcting the trial values until the residuals are reduced to a suitable tolerance level. This is usually accomplished in one or two iterations through use of linear extrapolation for the first trial values. If the Newton-Raphson corrections are applied only once, i.e., there is no iteration, the non-linear system of difference equations degenerates to the equivalent of a quasi-linear formulation which may require smaller time steps than the non-linear formulation for the same degree of numerical accuracy.

A system of 2N x 2N linear equations relates the corrections to the residuals and to a Jacobian coefficient matrix composed of partial derivatives of each equation with respect to each unknown variable in that equation. The coefficient matrix of the linear system has a banded

structure which allows the system to be solved by a compact quad-diagonal Gaussian elimination algorithm (Fread, 1971), which is very efficient with respect to computing time and storage. The required storage is 2N x 4 and the required number of computational steps is approximately 38N.

The DAMBRK model has the option to use either equation (22)-(23) or equations (26)-(27). The former is a somewhat simpler treatment in which a total or composite cross-section is used, whereas the latter set utilizes a more detailed representation of the flow cross-section. Eqs. (26)-(27) are recommended when the channel is sufficiently large to carry a significant portion of the total flow and the channel has a rather meandrous path through the downstream valley.

In order to solve the unsteady flow equations the state of the flow (h and Q) must be known at all cross-sections at the beginning (t=0) of the simulation. This is known as the initial condition of the flow. The DAMBRK model assumes the flow to be steady, non-uniform flow where the flow at each cross-section is initially computed to be:

$$Q_i = Q_{i-1} + q_{i-1}\,\Delta x_{i-1} \qquad i=2,3,\ldots N \tag{47}$$

where Q_1 is the known steady discharge at the dam, i.e., the upstream boundary of the downstream valley, and q_i is any lateral inflow from tributaries existing between the cross-sections spaced at intervals of Δx along the valley. The steady discharge from the dam at t=0 must be non-zero, i.e., a dry downstream channel is not amenable to simulation by DAMBRK. This is not an important restriction, especially when maximum flows and peak stages are of paramount interest in the dam-break flood. The tributary lateral inflow must be specified by the forecaster throughout the simulation period. If these flows are relatively small, they may be safely ignored.

The water surface elevations associated with the steady flow must also be computed at t=0. This is accomplished by solving the following equation:

$$\frac{(Q^2/A)_{i+1} - (Q^2/A)_i}{\Delta x_i} + g\left[\frac{A_i+A_{i+1}}{2}\right]\left[\frac{h_{i+1}-h_i}{\Delta x_i}\right.$$

$$\left.\frac{n^2(Q_i+Q_{i+1})^2\,(B_i+B_{i+1})^{4/3}}{2.2\,(A_i+A_{i+1})^{10/3}}\right] = 0 \tag{48}$$

This equation may be easily solved using the Newton-Raphson method by starting at a specified elevation at the downstream extremity of the

valley and solving for the adjacent upstream elevation step by step until the upstream boundary is reached. The downstream specified elevation may be obtained from a solution of the Manning equation if the flow is governed only by the channel conditions; however, if a flow control structure produces a back-up of the flow at this location, the forecaster must directly specify the water surface elevation existing at the downstream boundary at t=0.

In addition to initial conditions, boundary conditions at the upstream and downstream sections of the valley must be specified for all times (t=0 to t=t_e where t_e is the future time at which the simulation ceases).

At the upstream boundary the reservoir outflow hydrograph Q(t) provides the necessary boundary condition.

At the downstream boundary an appropriate stage-discharge relation is used. If the flow at the downstream extremity is channel-controlled, the following relation is used:

$$Q_N = \frac{1.49}{n} A_N^{5/3} / B_N^{2/3} \cdot \left[\frac{h_{N-1} - h_N}{\Delta x_{N-1}}\right]^{1/2} \qquad (49)$$

Equation (49) reproduces the hysteresis effect in stage-discharge relations often observed as a loop-rating curve. The loop (hysteresis) is produced by the temporal variations in the water surface slope. If the flow at the downstream boundary is controlled by a flow control structure such as a dam, the following relation is used:

$$Q_N = Q_b + Q_s \qquad (50)$$

where the breach flow (Q_b) is defined by equation (2) and the spillway flow (Q_s) is defined by equation (17) in which the various terms apply to the dam at the downstream boundary. Since the resulting expressions for Q_b and Q_s are in terms of the water surface elevation, h_N, equation (50) is a stage-discharge relation.

The downstream boundary condition may also be specified as a single-value rating curve in which the stage-discharge values are input as tabular values. Linear interpolation is used for determining intermediate values. The downstream boundary may also be a known water surface elevation as a function of time, e.g., a tidal condition.

1.5 Multiple Dams and Bridges

The DAMBRK model can simulate the progression of a dam-break wave through a downstream valley containing a reservoir created by another downstream dam, which itself may fail due to being sufficiently overtopped by the wave produced by the failure of the upstream dam. In fact, an unlimited number of reservoirs located sequentially along the

valley can be simulated. In DAMBRK there is a choice of two methods for simulating dam-break flows in a valley having multiple dams.

In the first method, which is known as the "sequential method," the downstream boundary condition for the dynamic routing component is given by equation (50) rather than equation (49). The properties of the downstream dam, spillways, breach description, and elevation of flow which precipitates the failure of the dam, are used in Eq. (50). In this way, backwater effects of the downstream dam are included in the routing of the outflow hydrograph from the upstream dam. The most upstream reservoir may be simulated using either storage or dynamic routing.

When the tailwater below a dam is affected by flow conditions downstream of the tailwater section (e.g., backwater produced by a downstream dam, flow constriction, bridge, and/or tributary inflow), the flow occurring at the dam is computed by the second method known as the "simultaneous method" which uses an internal boundary condition at the dam. In this method the dam is treated as a short Δx reach in which the flow through the reach is governed by the following two equations rather than either equation (22)-(23) or equations (26)-(27):

$$Q_i = Q_{i+1} \tag{51}$$

$$Q_i = Q_b + Q_s \tag{52}$$

in which Q_b and Q_s are breach flow and spillway flow as described in equation (2) and (17). In this way the flows, Q_i and Q_{i+1}, and the elevations, h_i and h_{i+1}, are in balance with the other flows and elevations occurring simultaneously throughout the entire flow system; the system may consist of additional dams which are treated as additional internal boundary conditions via Eqs. (51)-(52). Either storage or dynamic routing may be used in the most upstream reservoir. This method can also be used for a flow system having a single dam, only.

Highway/railway bridges and their associated earthen embankments which are located at points downstream of a dam may also be treated as internal boundary conditions. Equations (51)-(52) are used at each bridge; the term Q_s in equation (52) is computed by the following expression:

$$Q_s = 8.02\, C\, A_{i+1}(h_i - h_{i+1})^{1/2} + cc_u\, L_u\, k_u (h_i - h_{cu})^{3/2} + cc_\ell\, L_\ell\, k_\ell (h_i - h_{c\ell})^{3/2} \tag{53}$$

in which

$$k_u = 1.0 \qquad \text{if} \quad h_{ru} \leq 0.76 \tag{54}$$

$$k_u = 1.0 - c_u(h_{ru} - 0.76)^3 \quad \text{if} \quad h_{ru} > 0.76 \tag{55}$$

$$c_u = 133(h_{ru}-0.78) + 10 \quad \text{if} \quad 0.76 \leq h_{ru} \leq 0.96 \tag{56}$$

$$c_u = 400(h_{ru}-0.96) + 34 \quad \text{if} \quad h_{ru} > 0.96 \tag{57}$$

$$h_{ru} = (h_{i+1}-h_{cu})/(h_i-h_{cu}) \tag{58}$$

$$cc_u = 3.02(h_i-h_{cu})^{0.015} \quad \text{if} \quad 0 < h_u \leq 0.15 \tag{59}$$

$$cc_u = 3.06 + 0.27(h_u-0.15) \quad \text{if} \quad h_u > 0.15 \tag{60}$$

$$h_u = (h_i-h_{cu})/w_u \tag{61}$$

in which C is a coefficient of bridge flow (see Chow, 1959), A_{i+1} is the cross-section flow area of the bridge opening at section i+1 (downstream end of bridge), h_{cu} is the elevation of the upper embankment crest, h_i is the water surface elevation at section i (upstream end of bridge), h_{i+1} is the water surface elevation at section i+1, L_u is the length of the upper embankment crest perpendicular to flow direction), k_u is the submergence correction factor for flow over the upper embankment crest, and w_u is the width (parallel to flow direction) of the crest of the upper embankment. In Eq. (53), the terms with an (ℓ) subscript refer to a lower embankment crest and these terms are defined by equations (54)-(61) in which the (u) subscripts are replaced with (ℓ) subscripts. Equations (54)-(61) were developed from basic information on flow over road embankments as reported by the U.S. Dept. of Transportation (1978).

1.6 Supercritical Flow

The DAMBRK model can simulate the flow through the downstream valley when the flow is supercritical. This type of flow occurs when the slope of the downstream valley exceeds about 50 ft/mi. Slopes less than this usually result in the flow being subcritical to which all preceding comments pertaining to the downstream routing apply. When the flow is supercritical, any flow disturbances cannot travel back upstream; therefore, the downstream boundary becomes superfluous. Thus, for supercritical flow, a downstream boundary condition is not required; however, another equation in addition to the reservoir outflow hydrograph is needed for the upstream boundary condition. To satisfy this requirement, an equation similar to equation (49) is used at the upstream boundary, i.e.,

$$Q_1 = \frac{1.486}{n} A_1^{5/3}/B_1^{5/3} \left[\frac{h_1-h_2}{\Delta x_1}\right]^{1/2} \tag{62}$$

A modified compact quad-diagonal Gaussian elimination algorithm similar to the one previously described is required for solving the unsteady flow equations when supercritical flow exists. The modification results when the form of the Jacobian coefficient matrix is slightly changed due to the need for two upstream boundary conditions and none at the downstream boundary.

The DAMBRK model is constructed to accommodate supercritical flow for either the entire channel reach or for only an upstream portion of the entire reach. The supercritical flow regime is assumed to be applicable throughout the duration of the flow. Multiple reservoirs on supercritical valley slopes must be treated using a storage routing technique such as equation (18) rather than the dynamic routing technique.

1.7 Routing Losses

Often in the case of dam-break floods, where the extremely high flows inundate considerable portions of channel overbank or valley flood plain, a measurable loss of flow volume occurs. This is due to infiltration into the relatively dry overbank material, detention storage losses, and sometimes short-circuiting of flows from the main valley into other drainage basins via canals or overtopping natural ridges separating the drainage basins. Such losses of flow may be taken into account via the term q in equation (22) or equation (26). An expression describing the loss is given by the following:

$$q_m = -0.00458\ V_L\ P/(L\ \bar{T}) \tag{63}$$

in which V_L is the outflow volume (acre-ft) from the reservoir; P is the volume loss ratio; L is the length (mi) of downstream channel through which the loss occurs; and T is the average duration (hr) of the flood wave throughout the reach length L; and q_m is the maximum lateral outflow (cfs/ft) occurring along the reach L throughout the duration of flow. The mean lateral outflow is proportioned in time and distance along the reach L such that $q_i^j=0$ when $Q_i^j=Q_i^1$ and $q_i^j=q_m$ when $Q_i^j=Q_{max_i}$. Thus:

$$q_i^j = \frac{(Q_i^j - Q_i^1)}{(Q_{max_i} - Q_i^1)}\ q_m \tag{64}$$

$$Q_{max_i} = Q_{max_N} + (Q_{max} - Q_{max_N})\ \left(\frac{X_N - X_i}{L}\right)^m \tag{65}$$

where Q_i^1 is the initial flow, Q_{max_i} is the estimated maximum flow at each flood node, Q_{max_N} is the maximum routed discharge at the downstream section (X_n), Q_{max} is the maximum discharge at the dam and m is a fitted

exponent. The parameter P may vary from only a few percent to more than 30, depending on the conditions of the downstream valley.

1.8 Tributary Inflows/Outflows

Unsteady flows associated with tributaries downstream of the dam can be added to the unsteady flow resulting from the dam failure. This is accomplished via the term q in equation(22) or equation(26). The tributary flow is distributed along a single Δx reach. Backwater effects of the dam-break flow on the tributary flow are ignored, and the tributary flow is assumed to enter perpendicular to the dam-break flow. Outflows are assigned negative values. Outflows which occur as broad-crested weir flow over a levee or natural crest may be simulated. The crest elevation, discharge coefficient, and location along the river-valley must be specified. The head is computed as the average water surface elevation, along the length of the crest, less the crest elevation.

1.9 Floodplain Compartments

The DAMBRK model can simulate the exchange of flow between the river and floodplain compartments. The floodplain compartments are formed by a levee which runs parallel to the river on either or both sides of the river, and other levees or road embankments which run perpendicular to the river. Flow transfer between a floodplain compartment and the river is assumed to occur along one Δx reach and is controlled by broad-crested weir flow with submergence correction. Flow can be either away from the river or into the river, depending on the relative water surface elevations of the river and the floodplain compartment. The river elevations are computed via equation(40-41), and the floodplain water surface elevations are computed by a simple storage routing relation, i.e.,

$$V_\ell^t = V_\ell^{t-\Delta t} + (I^t - O^t)\ \Delta t/43560 \qquad (66)$$

in which V_ℓ is the volume (acre-ft) in the floodplain compartment at time t or $t-\Delta t$ referenced to the water elevation, I is the inflow from the river or adjacent floodplain compartments, and O is the outflow from the floodplain compartment to the river and/or to adjacent floodplain compartments. Flow transfer between adjacent floodplain compartments is also controlled by broad-crested weir flow with submergence correction. The broad-crested weir flow is according to the following:

$$I = c\ s_b\ (h_r - h_{fp})^{3/2} \qquad (67)$$

$$O = c\ s_b\ (h_{fp} - h_r)^{3/2} \qquad (68)$$

in which c is a specified discharge coefficient, h_r is the river elevation, h_{fp} is the water surface elevation of the floodplain, and s_b is the submergence correction factor, i.e.

$$s_b = 1.0 \qquad h_r < 0.67 \tag{69}$$

$$s_b = 1.0 - 27.8\,(H_r - 0.67)^3 \qquad h_r > 0.67 \tag{70}$$

$$H_r = (h_r - h_w)/(h_{fp} - h_w) \tag{71}$$

and h_w is the specified elevation of the crest of the levee. The floodplain elevation (h_{fp}) is obtained iteratively via a table look-up algorithm from the specified table of volume-elevation values. The outflow from a floodplain compartment may also include that from one or more pumps associated with each floodplain compartment. Each pump has a specified discharge-head relation given in tabular form along with start-up and shut-off operation instructions depending on specified water surface elevations. The pumps discharge to the river.

1.10 Reservoir Dynamic Routing

As mentioned earlier, an option is provided in the DAMBRK model to use dynamic routing rather than storage routing to compute the reservoir outflow hydrograph. The dynamic routing is identical to the above description with the exception of boundary conditions. The upstream boundary condition is a discharge hydrograph given by the following:

$$Q_1^{j+1} - I(t) = 0 \tag{72}$$

where I(t) is the known reservoir inflow hydrograph. The downstream boundary condition is a stage-discharge relation given by equation (50). The initial water surface elevations are computed by solving equation (48), the steady gradually varied backwater equation, using h_o which is the elevation of the water surface at the dam site when the computation commences. The reservoir dynamic routing procedure must contend with the lowering of the water surface elevation at the upstream boundary as the reservoir volume is depleted by the outflow through the breach. If this depth becomes small and approaches a value less than the normal depth, the computations become unstable. To avoid this computational problem, the upstream depth is constantly monitored; if it becomes less than the initial normal depth (d_n), the location of the upstream boundary condition is shifted downstream one node at a time until the depth at the node is greater than d_n.

1.11 Landslide-Generated Waves

Reservoirs are sometimes subject to landslides which rush into the reservoir, displacing a portion of the reservoir contents and, thereby,

creating a very steep water wave which travels up and down the length of the reservoir (Davidson and McCartney, 1975). This wave may have sufficient amplitude to overtop the dam and precipitate a failure of the dam, or the wave by itself may be large enough to cause catastrophic flooding downstream of the dam without resulting in the failure of the dam as perhaps in the case of a concrete dam such as the Vlaont Dam flood of 1963.

The capability to generate waves produced by landslides is provided within DAMBRK. The volume of the landslide mass, its porosity, and time interval over which the landslide occurs, are input to the model. In the model, the landslide mass is deposited within the reservoir in layers during small computational time steps, and simultaneously the original dimensions of the reservoir are reduced accordingly. The time rate of reduction in the reservoir cross-sectional area (Koutitas, 1977) creates the wave during the solution of the unsteady flow, equation (22)-(23), which are applied to the cross-sections describing the reservoir characteristics. The upstream boundary condition is given by equation (72), and the downstream boundary condition is given by equation (50). The initial conditions are obtained as described by equations (47)-(48) for steady non-uniform flow.

Wave runup is not considered in the model. For near vertical faces of concrete dams the runup may be neglected; however, for earthen dams the angle of the earth fill on the reservoir side will result in a surge which will advance up the face of the dam to a height approximately equal to 2.5 times the height of the landslide-generated wave (Morris and Wiggert, 1972).

1.12 Selection of Δt and Δx

Rapidly rising hydrographs, such as the dam-break outflow hydrograph, can cause computational problems (instability and non-convergence) when applied to numerical approximations of the unsteady flow equations. This is the case even when an implicit, non-linear finite difference solution technique is used. However, many computational problems can be overcome by proper selection of time step (Δt) size. During the limited testing of the model presented herein, two types of computational problems arose. First, if the time step were too large relative to the rate of increase of discharge during that time step, errors occurred in the computed water surface elevation in the vicinity of the wave front. These water surface elevations would tend to dip toward the channel bottom and quickly cause negative areas to be computed which would then cause the computations to "blow up." Second, too large a time step would also cause the Newton-Raphson iteration to not converge. The first computational problem is similar to that experienced by Cunge (1975). Both of the computational problems were successfully treated by reducing the time step size by a factor of 0.5 whenever negative areas were computed, or when a reasonable number of iterations were exceeded. With the reduced time step, the computations were repeated. If the same problems persisted, the time step was again halved and the computations repeated. Usually, one or two reductions

would be sufficient. The computational process was then advanced to the next time level by the original unreduced time step. Computations were initially begun with Δt time steps (hr) computed via the following relation:

$$\Delta t = \tau/M \tag{73}$$

in which τ is the time (hr) from the beginning of rise to the peak of the outflow hydrograph and M is the divisor for determining the time step. A reasonable value for M is 20 for subcritical flow and 40 for supercritical flow.

Distance steps (Δx) are selected in the following range:

$$\Delta x \leq c\ \Delta t \tag{74}$$

where c is the wave speed in mi/hr and Δx is in miles. The dam-break hydrograph tends to be a very peaked-type of hydrograph and, as such, tends to dampen and flatten out as it advances downstream. Accordingly, the time step may be increased as the wave progresses downstream; therefore, smaller values of Δx are selected immediately downstream of the dam, with a gradual increase in size at greater distances downstream of the dam. Also, the smaller values of Δx are associated with the smaller values of τ. This methodology of selecting Δx and Δt values follows the guidelines set forth in an analysis made by Fread (1974a) of the numerical properties of the four-point implicit solution of the unsteady flow equations.

Distance steps may need to be reduced in size where severe expansions or contractions in the cross sections occur.

Since the flood wave dampens out as it moves downstream, the Δt time step may be increased as the computations advance in time. The following scheme is used:

$$\Delta t = T_p/M \qquad t \leq t_b + 2\tau \tag{75}$$

where T_p is the time between the start of rise of the hydrograph and the peak of the hydrograph at selected locations along the downstream valley. Six evenly spaced locations along the downstream valley commencing at the dam site are monitored to determine T_p. The peak must have occurred at one of the locations before T_p can be evaluated. Since T_p increases at locations farther and farther downstream of the dam, the T_p which exists for the most downstream location is used in equation (75). An option exists to maintain throughout the computations and time step size specified in the data input. The units of Δt, t_b, and T_p are hours.

REFERENCES

Amein, M., and C. S. Fang, 1970: Implicit flood routing in natural channels. Journ. Hydraulic. Div., ASCE, 96, HY12, Dec., pp. 2481-2500.

Balloffet, A., 1977: Simulation of dam break flooding under normal and probable maximum flood conditions, Proceedings, Dam-Break Flood Modeling Workshop, U. S. Water Resources Council, Washington, D.C., pp. 384-401.

Balloffet, A., E. Cole, and A. F. Balloffet, 1974: Dam collapse wave in a river, Journ. Hydraul. Div., ASCE, 100, HY5, May, pp. 645-665.

Baltzer, R., and C. Lai, 1969: Computer simulation of unsteady flows in waterways. Journ. Hydraul. Div., ASCE, 94, HY4, July, pp. 1083-1117.

Brater, E., 1959: Hydraulics. Civil Engineering Handbook, edited by L. C. Urquhart, Sect. 4, McGraw-Hill Book Co., New York, pp. 4.44-4.60.

Brevard, J. A., and F. D. Theurer, 1979: Simplified dam-break routing procedure, Technical Release Number 66, U. S. Dept. of Agriculture, Soil Conservation Service, Engr. Div., 35 pp.

Brown, R. J., and D. C. Rogers, 1977: A simulation of the hydraulic events during and following the Teton Dam failure, Proceedings, Dam-Break Flood Modeling Workshop, U. S. Water Resources Council, Washington, D. C. pp.131-163.

Chaudhry, Y. M., and D. N. Contractor, 1973: Application of the implicit method to surges in open channels. Water Resour. Res., 9, No. 6, Dec., pp. 1605-1612.

Chen, C., and L. A. Druffel, 1977: Dam-break flood wave computation by method of characteristics and linearized implicit schemes, Proceedings, Dam-Break Flood Modeling Workshop, U. S. Water Resources Council, Washington, D. C., pp. 312-345.

Chow, V. T., 1959: Open-channel Hydraulics, McGraw-Hill Co., New York, pp. 476-481.

Cristofano, E. A., 1965: Method of computing rate for failure of earth fill dams. Bureau of Reclamation, Denver, Colo., April.

Cunge, J. A., 1975: Rapidly varying flow in power and pumping canals. Unsteady Flow in Open Channels, edited by K. Mahmood and V. Yevjevich, Vol. II, Chapt. 14, Water Resour. Pub., Ft. Collins, Colo., pp. 539-586.

Davidson, D. D., and B. L. McCartney, 1975; Water waves generated by landslides in reservoirs. Journ. Hydraul. Div., ASCE, 101, HY12, Dec., pp. 1489-1501.

Davies, W. E., J. F. Bailey, and D. B. Kelly, 1972: West Virginia's Buffalo Creek flood: a study of the hydrology and engineering geology. Geological Survey Circular 667, U. S. Geological Survey, 32 pp.

De Saint-Venant, Barre, 1871: Theory of unsteady water flow, with application to river floods and to propagation of tides in river channels. Acad. Sci. (Paris) Comptes rendus, 73, pp. 237-240.

Dressler, R. F., 1954: Comparison of theories and experiments for the hydraulic dam-break wave. Internat. Assoc. Sci. Pubs., 3, No. 38, pp. 319-328.

Fread, D. L., 1971: Discussion of implicit flood routing in natural channels. M. Amein and C. S. Fang. Journ. Hydraul. Div., ASCE, 97, HY7, July, pp.1156-1159.

Fread, D. L., and T. E. Harbaugh, 1973" Transient hydraulic simulation of breached earth dams, Journ. Hydraul. Div., ASCE, 99, HY1, Jan., pp 139-154.

Fread, D. L., 1974a: Numerical properties of implicit four-point finite difference equations of unsteady flow. NOAA Tech. Memo. NWS HYDRO-18, U. S. Dept of Commerce, NOAA, National Weather Service, 38 pp.

Fread, D. L., 1974b: Implicit dynamic routing of floods and surges in the Lower Mississippi. Presented at AGU Natl. Mtg., Wash., D. C., April, 26 pp.

Fread, D. L., 1975: Discussion of comparison of four numerical methods for flood routing, R. K. Price, Journ. Hydraul. Div., ASCE, 101, HY3, March, pp.565-567.

Fread, D. L., 1976: Flood routing in meandering rivers with flood plains, Proceedings. Rivers '76, Third Ann. Symp. of Waterways, Harbors and Coastal Eng. Div., ASCE, Vol. I, Aug., pp. 16-35.

Fread, D. L., 1977: The development and testing of a dam-break flood forecasting model, Proceedings, Dam-Break Flood Modeling Workshop, U. S. Water Resources Council, Washington, D. C., 1977, pp. 164-197.

Fread, D. L., 1978: NWS operational dynamic wave model, Verification of Mathematical and Physical Models in Hydraulic Engineering, Proceedings, 26th Annual Hydraulics Div. Specialty Conf., College Park, Md., Aug., pp.455-464.

Gundlach, D. L., and W. A. Thomas, 1977: Guidelines for calculating and routing a dam-break flood, Research Note No. 5, Corps of Engineers, U. S. Army, The Hydrologic Engr. Center, 50 pp.

Harris, G. W., and D. A. Wagner, 1967: Outflow from breached dams, Univ. of Utah.

Johnson, F. A., and P. Illes, 1976: A classification of dam failures, Water Power and Dam Construction, Dec., pp. 43-45.

Keefer, T. N., and R. K. Simons, 1977: Qualitative comparison of three dam-break routing models, Proceedings, Dam-Break Flood Modeling Workshop, U. S. Water Resources Council, Washington, D. C., pp.292-311.

Koutitas, C.G., 1977: Finite element approach to waves due to landslides, Journ. Hydraul. Div., ASCE, 103, HY9, Sept., pp. 1021-1029.

Liggett, J., and J. A. Cunge, 1975: Numerical methods of solution of the unsteady flow equations. Unsteady Flow in Open Channels, edited by K. Mahmood and V. Yevjevich, Vol. I, Chapt. 4, Water Resour. Pub., Ft. Collins, Colo., pp. 89-182.

Martin, C. S., and J. J. Zovne, 1971: Finite-difference simulation of bore propagation. Journal. Hydraul. Div. ASCE, 97, HY7, July, pp. 993-1010.

McQuivey, R. S., and T. N. Keefer, 1976: Application of simple dam break routing model. Proceedings, 16th Congress, IAHR, Sao Paulo, Brazil, July 27-August 1, 1975, Vol. 2, pp. 315-324.

Middlebrooks, T. A., 1952: Earth-dam practice in the United States, Centennial Transactions, ASCE, Paper No. 2620, pp. 697-722.

Morris, H. M., and J. M. Wiggert, 1972: Applied Hydraulics in Engineering, The Ronald Press Co., New York, pp. 570-573.

Preissmann, A., 1961: Propagatin of translatory waves in channels and rivers. Paper presented at First Congress of French Assoc. for Computation, Grenoble, Sept. 14-16, Proceedings, AFCAL, pp. 433-442.

Price, J. T., G. W. Lowe, and J. M. Garrison, 1977: Unsteady flow modeling of dam-break waves, Proceedings, Dam-Break Flood Modeling Workshop, U. S. Water Resources Council, Washington, D. C., pp. 90-130.

Rajar, R., 1978: Mathematical Simulation of dam-break flow, Journ. Hydraul. Div., ASCE, 104, HY7, July, pp. 1011-1026.

Ray, H. A., L. C. Kjelstrom, E. G. Crosthwaite, and W. H. Low, 1976: The flood in southeastern Idaho from the Teton Dam failure of June 5, 1976. Unpublished open file report, U. S. Geological Survey, Boise, Idaho.

Re, R., 1946: A study of sudden water release from a body of water to canal by the graphical method. Houille Blanche (France), No. 3, pp. 181-187.

Ritter, A., 1892: The propagation of water waves. Ver. Deutsch Ingenieure Zeitschr. (Berlin), 36, Pt. 2, No. 33, pp. 947-954.

Sakkas, J. G., and T. Strelkoff, 1973: Dam break flood in a prismatic dry channel, Journ. Hydraul. Div., ASCE, 99, HY12, Dec., pp. 2195-2216.

Schocklitsch, A., 1917: On waves created by dam breaches. Akad. Wiss. (Vienna) Proc., 126, Pt. 2A, pp. 1489-1514.

Smith, R. H., 1978: Development of a dynamic flood routing model for small meandering rivers. Ph.D. dissertation, Univ. Missouri-Rolla, 159 pp.

Stoker, J. J., 1957: Water Waves, Inter-Science Pub., New York, pp. 333-341.

Strelkoff, T., 1970: Numerical solution of Saint-Venant equations. Journ. Hydraul. Div., ASCE, 96, HY1, Jan., pp. 223-252.

Su, S. T., and A. H. Barnes, 1970: Geometric and frictional effects on sudden releases. Journ. Hydraul. Div., ASCE, 96, HY11, Nov., pp. 2185-2200.

Terzidis, G., and T. Strelkoff, 1970: Computation of open channel surges and shocks. Journ. Hydraul. Div., ASCE, 96, HY12, Dec., pp. 2581-2610.

Thomas, W. A., 1977: Calculating and routing of the Teton dam-break flood, Proceedings, Dam-Break Flood Modeling Workshop, U. S. Water Resources Council, Washington, D. C., pp. 198-227.

U. S. Army Corps of Engineers, 1960: Floods resulting from suddenly breached dams--conditions of minimum resistance, hydraulic model investigation. Misc. Paper 2-374, Report 1, WES, Feb., 176 pp.

U. S. Army Corps of Engineers, 1961: Floods resulting from suddenly breached dams--conditions of high resistance, hydraulic model investigation. Misc. Paper 2-374, Report 2, WES, Nov., 121 pp.

U. S. Army Corps of Engineers, 1975, National Program of Inspection of Dams, Bol. I-4, Dept. of the Army, Office of Chief of Engineers, Washington, D. C.

U. S. Dept. Transportation/Federal Highway Administration, 1978: Hydraulics of Bridge Waterways, Hydraulic Design Series No. 1, Washington, D. C., pp. 45-46.

Venard, J. K., 1954: Elementary Fluid Mechanics, John Wiley and Sons, New York, pp. 312-325.